Available online at www.sciencedirect.com
ScienceDirect
Precambrian Research 150 (2006) 49–72
Precambrian Research
www.elsevier.com/locate/precamres

$^{40}Ar/^{39}Ar$ thermochronology of the Pan-African Damara Orogen, Namibia, with implications for tectonothermal and geodynamic evolution

David R. Gray [a,*], David A. Foster [b], Ben Goscombe [c], Cees W. Passchier [d], Rudolph A.J. Trouw [e]

[a] *School of Earth Sciences, University of Melbourne, Melbourne, 3010 Vic., Australia*
[b] *School of Geological Sciences, University of Florida, Gainesville, FL 32611-2120, USA*
[c] *School of Earth and Environmental Sciences, The University of Adelaide, Adelaide, 5005, Australia*
[d] *Institut für Geoswissenschaften, JohannesGutenburg University, 55099 Mainz, Germany*
[e] *Instituto de Geociências, Universidade Federal do Rio de Janeiro, 21949-900 Rio de Janeiro, Brazil*

Received 31 October 2005; received in revised form 18 June 2006; accepted 18 July 2006

Abstract

Forty-three $^{40}Ar/^{39}Ar$ step-heating experiments on white mica, biotite, hornblende and whole rocks from the Damara Orogen, Namibia revise and refine the regional perspective on cooling, exhumation, and tectonic reactivation across the orogen. These data also document post-orogenic motion on major shear zones and the thermal effects of late-syn to post-tectonic granite intrusions. These data show regional cooling through temperatures of ~300–350 °C from 545 to 520 Ma in the Central Kaoko Zone, 530–510 Ma in the Eastern Kaoko Zone, and 495–480 Ma in the Southern Zone of the Damara Belt. Discordant $^{40}Ar/^{39}Ar$ age spectra relate to (1) partial resetting of K-Ar isotopic system in micas by late-stage activity in the major Kaoko Belt shear zones such as the Purros and Three Palms Mylonite Zones, giving apparent ages of 467 ± 6, 481 ± 3 and ~492 Ma, and (2) thermal effects from granitic plutions particularly in the Ugab Domain of the Southern Kaoko Belt (500–475 Ma) and in the granite-dominated Central Zone of the Damara Belt (490–460 Ma). Phyllites of the lower grade flank regions of the orogen record apparent $^{40}Ar/^{39}Ar$ mica crystallization ages of ~517 Ma (Eastern Kaoko Zone), ~526 Ma (Northern Zone, Damara Belt), and ~568–553 Ma (Southern Foreland Zone, Damara Belt). The Southern Foreland samples, however, are maximum ages, due to variable influence of detrital mica. Rates of cooling vary between zones within the Kaoko Belt. In the Central Kaoko Belt hornblende, biotite and white mica apparent $^{40}Ar/^{39}Ar$ ages are similar, suggestive of rapid cooling through the 300–550 °C temperature range, whereas in the Orogen Core or Western Kaoko Belt hornblende and biotite apparent ages are older than the white mica ages, because the white micas record the reactivation of the main structures. These data support models of diachronous deformation and metamorphism of the component parts of the orogen, and suggest that Pan-African orogenesis in the Damara is broadly bracketed between 580 and 500 Ma with final movements through 480 Ma, and spans through the terminal amalgamation of Gondwana in the Kuunga Orogeny through the initiation of subduction under the Gondwana continental margin.

Keywords: Pan-African orogenesis; Damara Orogen; $^{40}Ar/^{39}Ar$ thermochronology; Namibia

* Corresponding author. Tel.: +61 3 83446931; fax: +61 3 98866804.
E-mail addresses: drgray@unimelb.edu.au (D.R. Gray), dfoster@geology.ufl.edu (D.A. Foster), ben.goscombe@adelaide.edu.au (B. Goscombe), cpasschi@mail.uni-mainz-de (C.W. Passchier).
0301-9268/$ – see front matter © 2006 Elsevier B.V. All rights reserved.
doi:10.1016/j.precamres.2006.07.003

1. Introduction

The Pan-African Damara Orogen of southern Africa is the result of temporally distinct, high-angle and oblique convergence in different parts of what appears to be a three-pronged orogenic system (e.g., Coward, 1981, 1983). Made up of the Kaoko and Gariep transpressive coastal belts, as well as an inland Damara Belt (Fig. 1) the Damara Orogen records ocean closure about an apparent collisional triple junction during the Pan-African assembly of Gondwana (e.g., Prave, 1996; Trompette, 1997; Frimmel and Frank, 1998; Maloof, 2000; Hanson, 2003).

Previous geochronologic and thermochronologic studies in the Damara Orogen of Namibia (Fig. 1) have suggested complex deformational, metamorphic and cooling histories (e.g., Kröner, 1982; Ahrendt et al., 1983a; Frimmel and Frank, 1998; Franz et al., 1999). Kröner (1982) for example, argued for a polycyclic orogenic history from ~650 to 450 Ma, characterized by at least four tectono-thermal events; referred to as the Palmental (pre—650 Ma), Usakos (650–620 Ma), Salem (570–540 Ma) and Alaskite (520–450 Ma) events. Ahrendt et al. (1983b) also argued for polycyclic orogenic evolution, with distinct events at ~550 and ~460 Ma, and another at possibly at~650 Ma. This study attempts to resolve the number and nature of these events, as well as establish their possible distribution across the orogen.

Most of the earlier thermochronology in the Damara Orogen was by the K-Ar method applied to whole rock and partial mineral separates (e.g., Ahrendt et al., 1983a,b), but more recently $^{40}Ar/^{39}Ar$ investigations have been undertaken on the Gariep Belt (Frimmel and Frank, 1998) and part of the Southern Zone (Kukla, 1993) to provide more refined age constraints.

This paper presents new $^{40}Ar/^{39}Ar$ thermochronologic and geochronologic data for the Kaoko Belt, the Ugab Zone at the juncture of the Kaoko and Damara Belts, and the Damara Belt. These data are used to further constrain the timing of regional deformation, cooling and exhumation, and to investigate the thermal history for the Damara Orogen. The results are integrated with recently published geochronological data on metamorphism and plutonism, and used firstly to refine the current orogenic framework and secondly to provide a revised tectonic evolution for the Namibian part of the Damara Orogen.

2. Geological background

Each of the belts that make up the Damara Orogen shows different deformational styles, types of shortening geometries and crustal architecture (Figs. 2 and 3). Structural grain is NNW-trending in the Kaoko and Gariep Belts, but is NE-trending in the Damara Belt (Fig. 3). Post-tectonic granites are largely confined to the Central and Northern Zones of the Damara Belt or Inland Branch (Fig. 1).

The Kaoko Belt (Figs. 3 and 4) is dominated by two major, sinistral strike-slip shear zones within high-grade amphibolite facies Damara Supergroup turbidites, incorporating basement slivers and sheared Pan-African age granitoids (Dürr and Dingeldey, 1996; Passchier et al., 2002; Goscombe et al., 2003a,b; Konopásek et al., 2004). It has half-flower structure geometry (Fig. 2a) with basement-cored fold-nappes, metamorphosed under intermediate-T/intermediate-P metamorphic conditions, extruded and thrust over the Congo craton (Dürr and Dingeldey, 1996; Goscombe et al., 2003a,b). The Kaoko Belt was metamorphosed at high average thermal gradient (30–38 °C/km) at conditions ranging from lower amphibolite facies 575 °C and 5.2 kbar to granulite facies 775 °C and 8 kbar (Goscombe et al., 2003b, 2005a; Konopásek et al., 2004).

In contrast the Gariep Belt (Fig. 1) is mostly of low-metamorphic grade (Frimmel, 1995, 2000a), consisting of an arcuate belt of SW-vergent, stacked oceanic thrust-sheets including mélange, metagreywacke turbidites and metabasalts, thrust over the passive continental margin of the Kalahari craton (Davies and Coward, 1982; Frimmel, 1995; Hälbich and Alchin, 1995). The Gariep Belt geometry (Fig. 2b) is a composite, obducted ophiolite thrust-nappe, overlying imbricate faults in the passive margin sequence (Von Veh, 1983 in Frimmel, 1995). Arcuate shear zones define the major boundaries in the Gariep Belt (Fig. 2) and show evidence of sinistral transpression (Davies and Coward, 1982; Gresse, 1994). Peak metamorphic conditions in the passive continental margin units (Port Nolloth Zone) is 520 °C and 3–3.5 kbar (Frimmel, 2000a), whereas the oceanic thrust sheets show an amphibolite facies metamorphism of 500–600 °C and 4–6 kbar overprinted by a lower greenschist facies metamorphism of 300–400 °C and 2–3 kbar (Frimmel and Hartnady, 1992; Frimmel, 2000a).

The Damara Belt (Figs. 1 and 2c) is an asymmetric, doubly vergent orogen (Coward, 1981, 1983; Miller, 1983). Deformation resulted from younger, high-angle convergence between the Congo and Kalahari cratrons (Coward, 1981; Miller, 1983; Porada et al., 1983). It shows pronounced structural zonation reflected by structural style and metamorphic grade variations (Fig. 3). The orogen asymmetry is defined by a wide zone of intense, N-dipping, shear-dominated fabrics and basement-cored fold-nappes along the southern part bordering the Kalahari craton (Fig. 2c), as well as

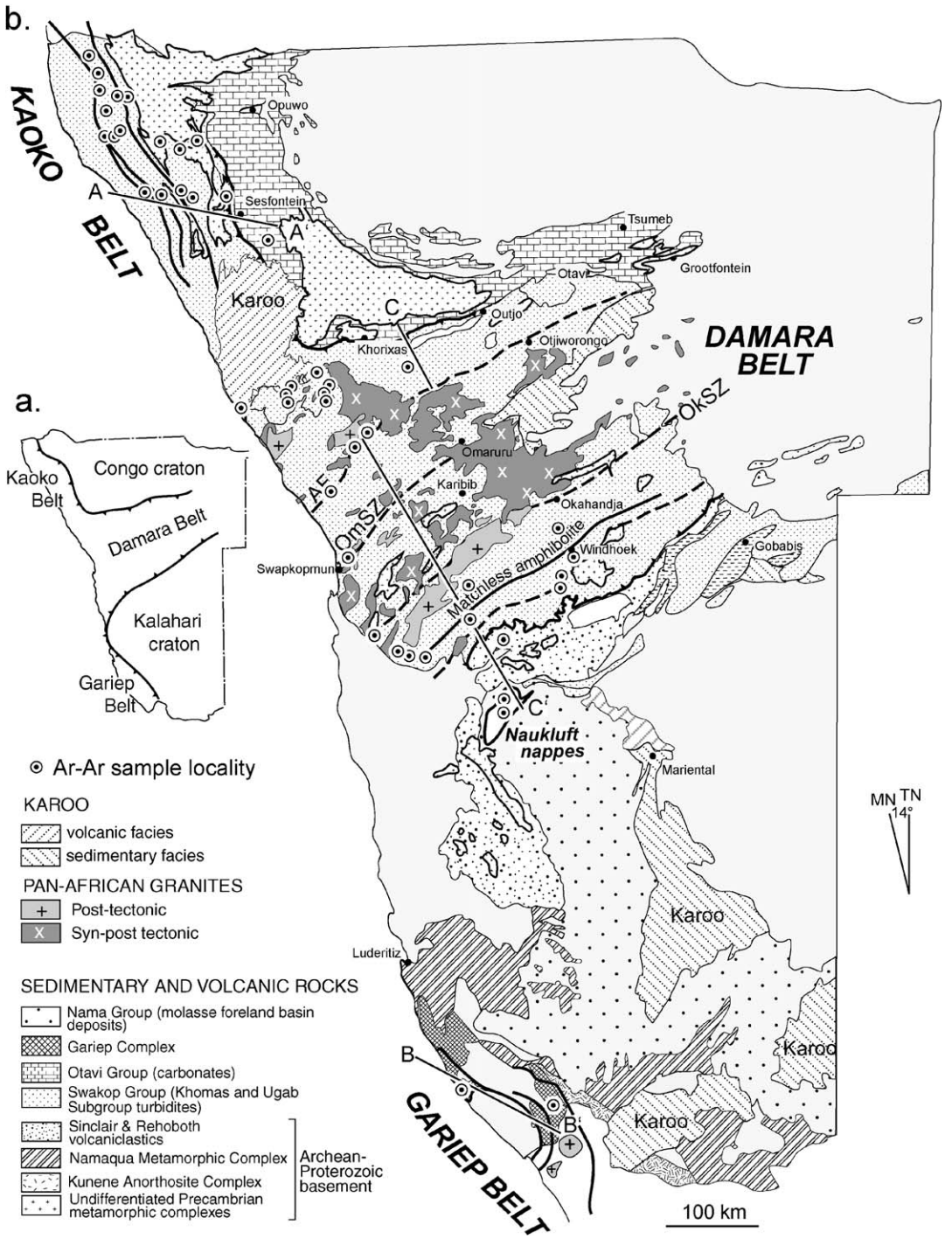

Fig. 1. (a) Simplified map showing the component arms or belts that define the collisional triple junction nature of the Damara Orogen, Namibia. (b) Geologic map of the Damara Orogen showing the main geological units, the major faults, and the distribution of plutonic rocks and Swakop Group turbidites (map modified from geological map of Namibia). Locations of the $^{40}Ar/^{39}Ar$ samples are shown. AF: Autseib Fault; OmSZ: Omaruru Shear Zone; OkSZ: Okahandja Shear Zone.

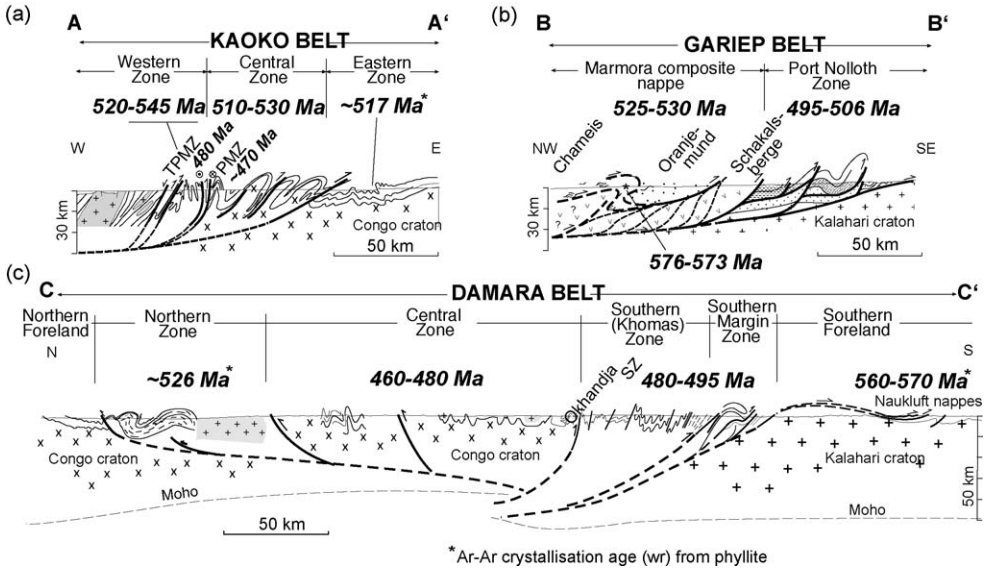

Fig. 2. Structural profiles across the Kaoko, Gariep and Damara Belts of the Damara Orogen. (a) Crustal architecture of the Kaoko Belt (modified from Goscombe et al., 2003a). (b) Crustal architecture of the Gariep Belt (modified from Von Veh, 1983 in Frimmel and Frank, 1998). (c) Crustal architecture of the Damara Belt (Inland or Intracontinental Branch) of the Damara Orogen (modified from Miller and Grote, 1988: profiles on Damara Orogen 1:500,000 Map sheets). Summaries of the $^{40}Ar/^{39}Ar$ data are shown across each profile. For location of the profile see Fig. 1.

an inner or Central Zone of granite-dominated, elongated, NW-trending basement cored domes and basins (Figs. 1–3). The Central Zone has garnet-cordierite-K-feldspar migmatitic granulites (e.g., Puhan, 1983; Masberg, 2000), indicating conditions of 720–850 °C and 4–6 kbar (Kasch, 1983a; Puhan, 1983), and shows a high average thermal gradient (30–50 °C/km). It contains A-type, post-tectonic granites that originate from mid-crustal, low pressure melting (McDermott et al., 2000). The marginal thrust belts reflect crustal thickening under intermediate-T/intermediate-P metamorphic conditions and separate the centrally located, granite-dominated, high-T/low-P metamorphic zone.

The junction between the Southern Kaoko Belt and the Damara Belt (Figs. 1 and 2) shows complex fold interference (Fig. 5) due to overprinting between N–S and E–W fold sets (Coward, 1983; Porada et al., 1983; Freyer and Hälbich, 1994; Maloof, 2000; Passchier et al., 2002; Goscombe et al., 2004). The Ugab Domain represents the southern extension of the Kaoko Belt and consists of chevron-folded turbidites formed in sinistral transpression (Passchier et al., 2002).

3. Previous geochronology/thermochronology

Apart from recent work in the Gariep Belt (Frimmel and Frank, 1998) and Kaoko Belt (Seth et al., 1998, 2000; Franz et al., 1999; Goscombe et al., 2003b, 2005b; Kröner et al., 2004), most of the Damara Orogen geochronology has been done on samples from the Damara Belt.

3.1. Damara Belt geochronology and thermochronology

The early geochronology of the Damara Belt comprised mainly K/Ar thermochronology and geochronology on whole rock samples and mineral concentrates undertaken by Clifford (1967), Haack and Hoffer (1976), Clauer and Kröner (1979), Kröner and Clauer (1979) and Ahrendt et al. (1977, 1983a,b), as well as Rb/Sr whole rock geochronology (Kröner, 1982; Hawkesworth et al., 1983). As summarized in Fig. 10 of Weber et al. (1983) these data showed:

(1) 410–470 Ma apparent ages for the Northern Zone (Kröner and Clauer, 1979; Ahrendt et al., 1983a,b).
(2) 430–496 Ma apparent ages in the southern part of the Central Zone (Clifford, 1967; Haack and Hoffer, 1976; Hawkesworth et al., 1983).
(3) 420–500 Ma apparent ages in the Southern Zone (Clifford, 1967; Haack and Hoffer, 1976; Hawkesworth et al., 1983).
(4) 495–530 Ma apparent ages for the Southern Margin Zone (Clifford, 1967; Weber et al., 1983).
(5) 500–550 Ma apparent ages for the Naukluft Nappes of the Southern Foreland (Ahrendt et al., 1977; Weber et al., 1983).

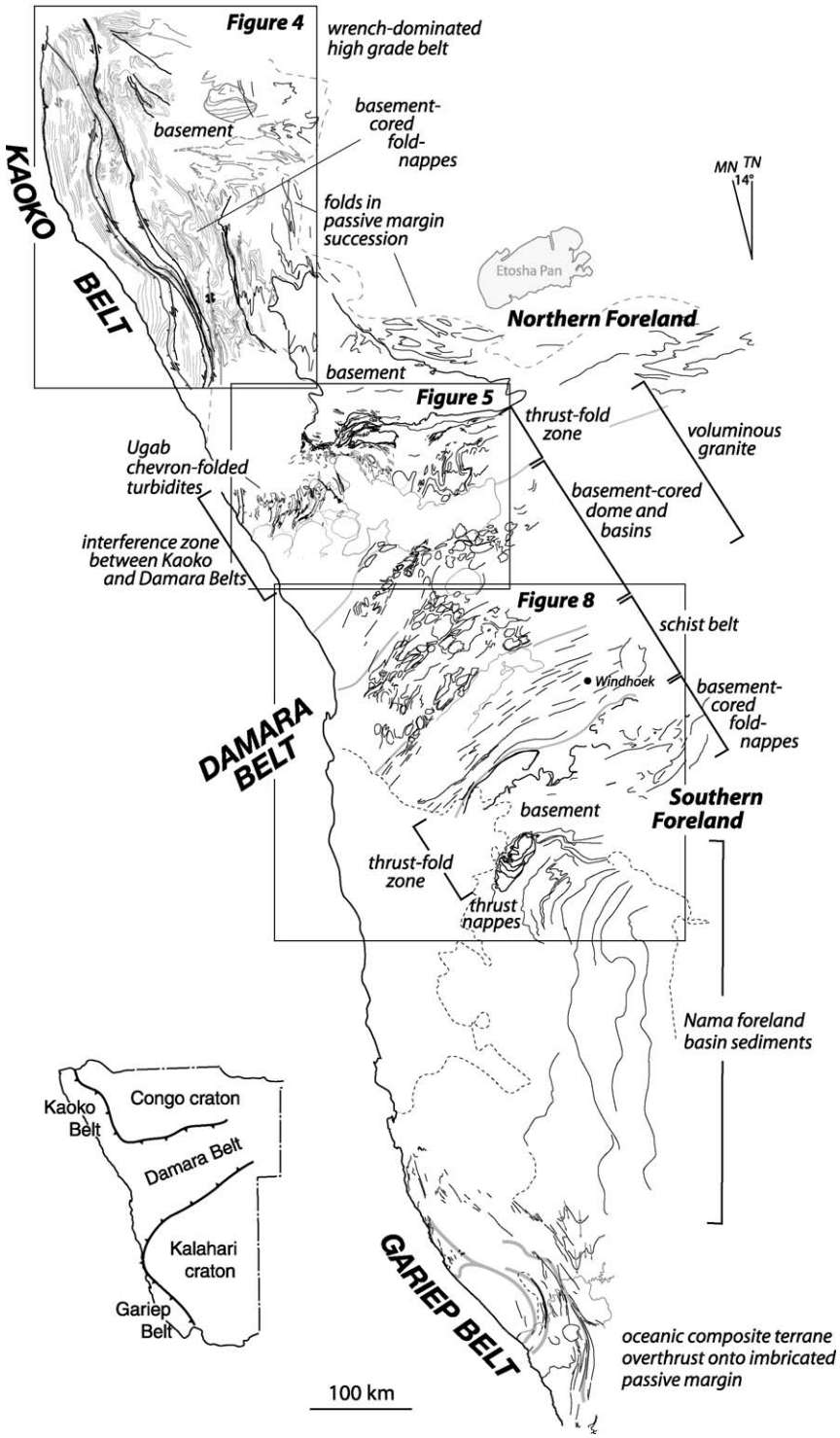

Fig. 3. Formline map of Namibia based on interpretation of the surface geology from NASA Satellite imagery (S-33-15, S-33-20 and S-33-25 image data files). The map shows the distinct structural style of the different belts or zones, as well as the style differences between the Kaoko, Gariep and Damara Belts within the Damara Orogen. The locations of Figs. 4–6 are shown.

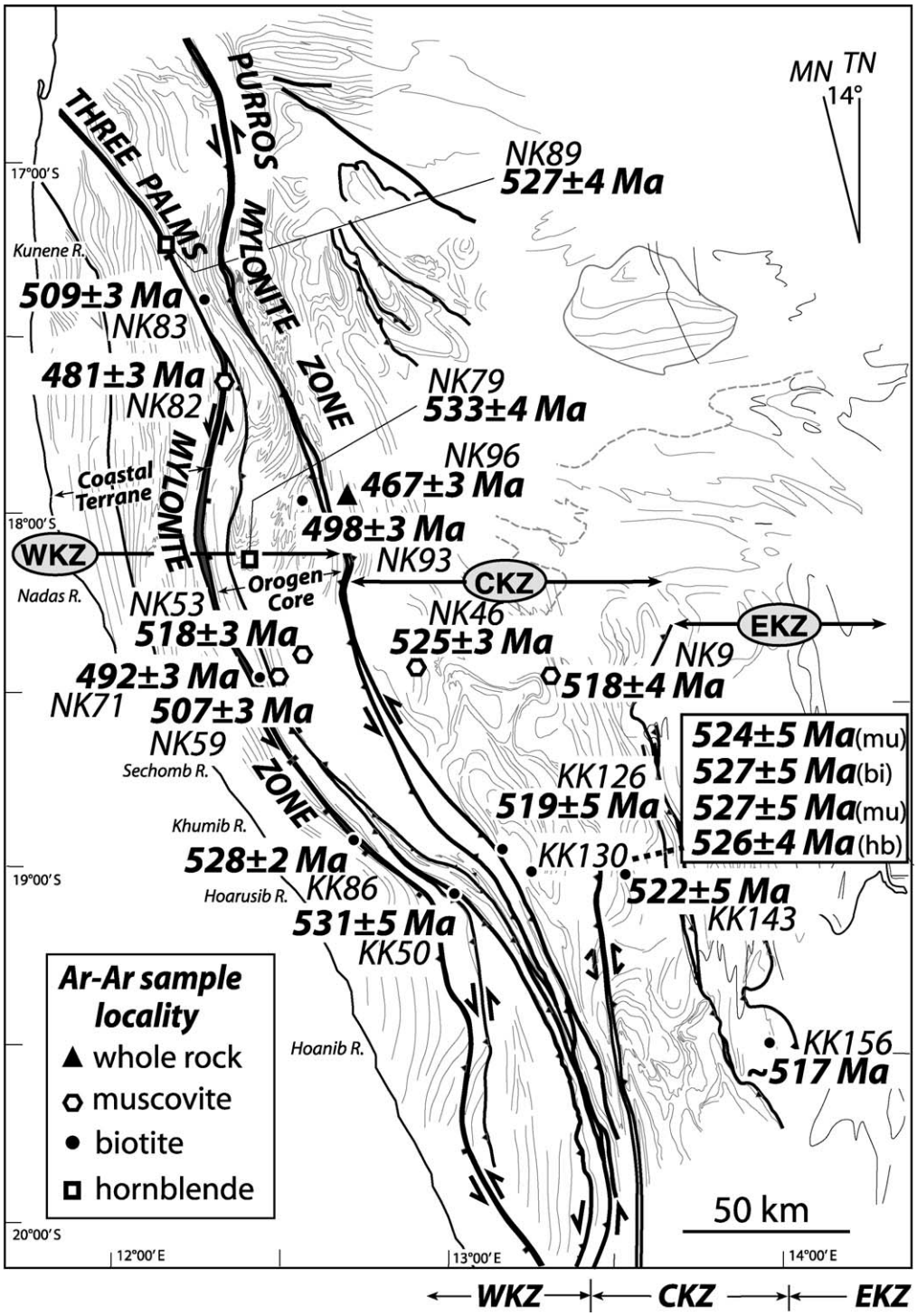

Fig. 4. $^{40}Ar/^{39}Ar$ data plotted on a formline structural map of the Kaoko Belt showing the major shear zones. WKZ: Western Kaoko Zone; CKZ: Central Kaoko Zone; EKZ: Eastern Kaoko Zone.

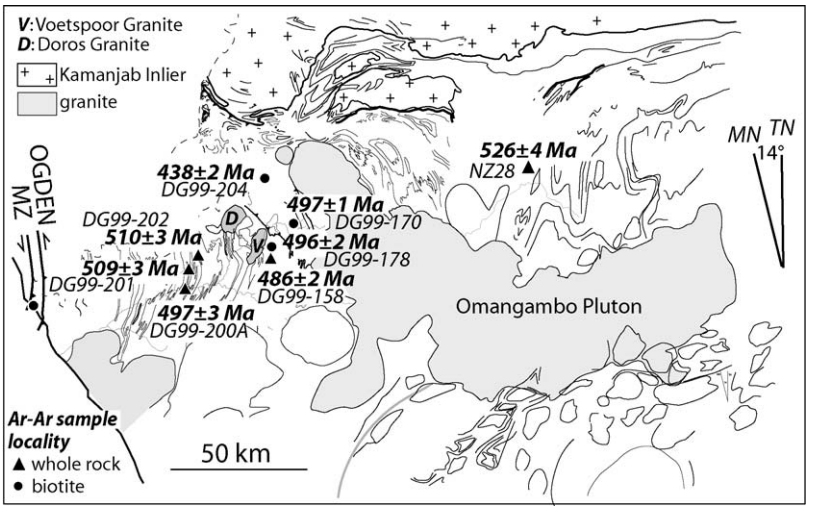

Fig. 5. $^{40}Ar/^{39}Ar$ data plotted on a formline structural map of the Ugab Zone (Southern Kaoko Belt) and western part of the Northern Zone (Damara Belt) representing the region of interference between Kaoko and Damara Belt deformation (base map from Miller and Grote, 1988 and NASA satellite imagery S-33-15). See Fig. 1 for location. Voetspoor (V) and Doros (D) Granites and the Omangambo Pluton are shown.

(6) 480–530 Ma for the Nama foreland basin (Ahrendt et al., 1983a).

The ages were generally interpreted as cooling ages reflecting a complex thermal history for the different parts of the orogen.

Rb/Sr biotite ages for the Central Zone range between 466 and 440 Ma (Haack and Hoffer, 1976; Hawkesworth et al., 1983; Tack and Bowden, 1999; Jung and Mezger, 2003). Haack and Hoffer (1976) ascribed these widespread ages in the internal parts of the Damara Belt to slow cooling and uplift following a single metamorphic event at ~520 Ma (cf. Haack et al., 1980; Haack, 1983). Kröner and Clauer (1979) inferred two low-grade regional tectono-thermal events at ~535 and 455 Ma, based on K/Ar dating of fine mineral fractions (<2 μm) from slates and phyllites from the Northern Zone of the Damara Belt. They suggested the widespread ages between 450 and 470 Ma in the Central Zone of the Damara Belt represented a tectono-thermal episode responsible for post-tectonic alaskitic granite emplacement. They also discussed the implications of an older event around 550–560 Ma. Kröner (1982) argued for a polycyclic orogenic history from ~650 to 450 Ma, characterized by at least four tectono-thermal events; referred to as the Palmental (pre—650 Ma), Usakos (650–620 Ma), Salem (570–540 Ma) and Alaskite (520–450 Ma) events.

Histograms of ages of the Damaran plutonic rocks (Fig. 48 of Miller, 1983) suggested three pulses of granitic magmatism at 650, 550 and 500 Ma. In contrast, monazite U/Pb growth ages from the Central Zone record three development stages at 540–530, 520–500 and 480–470 Ma (Briqueu et al., 1980; Kukla et al., 1991; Jung et al., 2000, 2001; Jung and Mezger, 2003). Concordance between Sm/Nd whole rock-garnet and U/Pb monazite ages from migmatites, metapelites and granites from the Central Zone suggest peak metamorphism between ~540 and 510 Ma but with a multistage growth history involving several stages of high-grade metamorphism related to intrusion of plutons (Jung and Mezger, 2003).

Early $^{40}Ar/^{39}Ar$ analyses were undertaken in the Central Zone by Hawkesworth et al. (1983), and more recently by Kukla (1993) for the Southern Zone who also undertook U/Pb monazite dating and Rb/Sr analysis of Kuiseb Schist. These data showed:

(1) Damara biotites have integrated $^{40}Ar/^{39}Ar$ ages similar to those determined by the Rb-Sr technique, with ages ranging from 508 to 460 Ma (Hawkesworth et al., 1983, pp. 331–332).
(2) Monazite ages form the Kuiseb Schist are between 518 and 513 Ma, whereas those from migmatite in the Schist between 525 and 515 Ma (Kukla, 1993, pp. 71–72) were interpreted as the peak of regional Kuiseb Schist metamorphism between 520 and 505 Ma.
(3) $^{40}Ar/^{39}Ar$ Kuiseb Schist biotite age of 490 ± 6 Ma, a biotite age of 485 ± 6 Ma and a muscovite age of 491 ± 6 Ma from Kuiseb Schist close to the Donkerhuk Granite (Kukla, 1993, p. 76).
(4) The ENE-trending post-tectonic Donkerhuk Granite intruded along the Okahandja Shear Zone

Table 1
Summary of Ar-Ar data

Sample[a]	Location	Lithology	Grid ref	Calculated age (Ma)[b]	Comments[c]
Kaoko Belt					
Western Kaoko					
NK89 (DG02-187) **hb**	Hartmann Valley	Mafic gneiss	S17°13.076′/E12°09.320′	***527 ± 4***	Plateau age, 68% of gas released
NK83 (DG02-182) bi	Hartmann Valley	Mylonitic orthogneiss	S17°28.503′/E12°15.819′	509 ± 3	Plateau age, 72% of gas released
NK82 (DG02-181) mu	Hartmann Valley	Mylonitic orthogneiss	S17°42.311′/E12°17.530’	481 ± 3	Plateau age, 70% of gas released
NK79 (DG02-179) **hb**	Hartmann Mtns	Mafic gneiss	S17°57.098′/E12°20.608′	***533 ± 4***	Plateau age, 91% of gas released
NK92 (DG02-189) mu	Nadas River Valley	Psammo-pelite sequence	S17°48.838′/E12°25.530′	498 ± 3	Plateau age, 95% of gas released
NK53 (DG02-158) mu	Nadas River Valley	Psammitic schist	S18°11.298′/E12°25.006′	518 ± 3	Plateau age, 85% of gas released
NK59 (DG02-162) mu	Nadas River Valley	Psammitic schist (garnet)	S18°11.989′/E12°23.279′	507 ± 3	Plateau age, 75% of gas released
NK71 (DG02-171) mu	Nadas River Valley	Mylonitised granite	S18°14.750′/E12°18.412′	492 ± 3	Plateau age, 90% of gas released
KK86 (DG01-112) (bi)	Khumib River Valley	Psammtic schist	S18°46.186′/E12°38.866′	528 ± 2	TFA
KK86 (DG01-112) hb	Khumib River Valley	Psammtic schist	S18°46.186′/E12°38.866′	565 ± 3	TFA, minimum age 548 ± 5 Ma
KK50 (DG01-90) (bi)	Hoarusib River Valley	Garnet-sillimanite gneiss	S18°51.245′/E12°52.754′	531 ± 5	Plateau age, 50% of gas released
Central Kaoko					
NK96 (DG02-193) wr	Red Drum, Marienfluss	Mylonitised schist	S17°47.814′/E12°31.300′	467 ± 3	“Error” plateau, 48% of gas released, argon loss gradient
NK46 (DG02-151) mu	Orumpembe	Biotite schist	S18°14.616′/E12°50.405′	525 ± 3	Plateau age, 75% of gas released
NK9 (DG02-116) mu	Otijiu, 90 km E of Opuwo	Muscovite schist	S18°16.436′/E13°12.472′	518 ± 4	Plateau age, 70% of gas released
KK126 (DG01-132A) (bi)	Gomatum Valley	Musc-Kspar-schistose gneiss	S18°47.489′/E13°01.120′	519 ± 5	Plateau age, 49% of gas released
KK130 (DG01-136a) mu	Gomatum Valley	Musc-biotite schist	S18°47.795′/E13°07.405′	524 ± 5	Plateau age, 98% of gas released
KK130 (DG01-136c) bi	Gomatum Valley	Musc-biotite schist	S18°47.795′/E13°07.405′	527 ± 5	Plateau age, 61% of gas released
KK130 (DG01-136c) mu	Gomatum Valley	Musc-biotite schist	S18°47.795′/E13°07.405′	527 ± 5	Plateau age, 95% of gas released
KK130 (DG01-136d) **hb**	Gomatum Valley	Amphibole schist	S18°47.795′/E13°07.405′	***526 ± 4***	Plateau age, 71% of gas released
KK143 (DG01-146) mu	Tsongwari Prospect	Phengitic schist	S18°47.493′/E13°25.447′	522 ± 5	Plateau age, 82% of gas released
Eastern Kaoko					
KK156 (DG01-158A) wr	Khowarib, E of Sesfontein	Phyllite	S19°15.726′/E13°52.260′	517 ± 2	Plateau age, 73% of gas released
Ugab Domain					
DG99-200 (wr)	Rhino Wash track	Phyllite	S20°54.477′/E14°04.362′	497 ± 3	TFA
DG99-201 (wr)	Rhino Wash track	Phyllite	S20°51.431′/E14°05.058′	509 ± 3	TFA
DG99-202 (wr)	Rhino Wash track	Phyllite	S20°50.517′/E14°05.983′	510 ± 3	TFA; plateau segment at 511 ± 2 Ma
DG99-204 (bi)	Twyfelfontein	Contact aureole schist	S20°36.720′/E14°21.641′	438 ± 2	TFA; age gradient due to argon loss
DG99-158 (wr)	E side Voetspoor granite	Contact aureole schist	S20°50.517′/E14°05.983′	486 ± 2	Plateau age, 60% of gas released

DG99-178 (bi)	E side Voetspoor granite	Contact aureole schist	S20°50.422′/E14°21.561′	496 ± 2	Plateau age, 50% of gas released
DG99-170 (bi)	Guantegab River	Mica quartzite	S20°45.316′/E14°25.632′	497 ± 1	Plateau age, 65% of gas released
U355 (**hb**)	E side of Ugab region	Amphibole schist	S20°54.431′/E14°32.543′	***513*** ± ***5***	Error plateau, 67% of gas released
Damara Belt					
Northern Zone					
NZ28 wr	Summas	Mica schist	S20°33.765′/E15°20.032′	526 ± 4	Error plateau, 78% of gas released
Central Zone					
CZ121 (bi)	Swakopmund	Mica schist	S 22°34.584′/E14°32.314′	480 ± 3	TFA
CZ50 mu	Kuiseb River	Mica schist	S 23°21.546′/E14° 53.237′	459 ± 4	Plateau segment, age gradient indicates argon loss
Southern Zone					
SZ29 mu	Kuiseb River	Mica schist	S23°35.057′/E15°06.547′	477 ± 3	Plateau age, 64% of gas released (saddle-shaped spectrum)
SZ40 (hb)	Garob Mine	Mica schist	S23°33.453′/E15°24.905′	505 ± 2	Plateau segment
SZ40 (bt)	Garob Mine	Mica schist	S23°33.453′/E15°24.905′	494 ± 5	Plateau age, 86% of gas released
SZ63 (mu)	Khomas Hochland	Mica schist	S23°04.987′/E15°46.873′	486 ± 3	Plateau age, 84% of gas released
SZ63 (bi)	Khomas Hochland	Mica schist	S23°04.987′/E15°46.873′	482 ± 4	Plateau age, 77% of gas released
DG01-66 (mu)	Okapuka Hill, N of Windhoek	Muscovite schist	S22°26.137′/E17°04.317′	496 ± 3	Plateau age, 70% of gas released
DG99-205B (bi)	Heinitzburg St, Windhoek	Mica schist	S22°34.535′/E17°05.524′	488 ± 3	
SZ78 (DG02-97) (mu)	C26Walvis Bay Rd	Garnet-biotite schist	S22°48.087′/E16°52.638′	495 ± 3	Plateau age, 80% of gas released
SZ87 (DG02-106) (mu)	C26Walvis Bay Rd	Biotite schist	S22°52.985′/E16°51.943′	495 ± 3	Plateau age, 85% of gas released
Southern Foreland					
DG03-169 wr	Bullsport, Naukluft Mtns	Green phyllite	S24°07.032′/E16°16.077′	568 ± 3	Plateau age, 64% of gas released
DG03-170 wr	Nauchus Rd, Naukluft Mtns	Grey phyllite	S23°57.592′/E16°14.357′	555 ± 3	Error plateau, 82% of gas released

Grid ref: map #/grid reference (based on 1:50,000 map series or 1:63,000 series where designated with an S).

[a] Picked white mica (mu), biotite (bi), oramphibole (hb), except where noted as whole rock (wr); bold text for data published in Goscombe et al. (2005b).

[b] Errors are one sigma.

[c] TFA = total fusion age.

between the Central and Southern Zones has a 505 ± 4 Ma magmatic monazite (U/Pb) age, along with Rb/Sr muscovite and biotite ages of 506 ± 7 and 492 ± 10 Ma, respectively (Kukla, 1993).

K/Ar dates and illite crystallinity determinations on phyllites and phyllitic slates from the Naukluft Nappe region by Ahrendt et al. (1977) show (1) two isochron ages of 530 and 495 Ma, with the peak metamorphism assumed to be at 530 Ma and nappe emplacement at 495 Ma, (2) an isochron age of 495 Ma from the basal mylonite zone or main thrust plane beneath the nappes, and (3) that the structurally highest thrust-nappe sheets had the highest metamorphic grade.

3.2. Kaoko Belt geochronology and thermochronology

K/Ar thermochronology by Ahrendt et al. (1983b) was the earliest work done in the Kaoko Belt. Samples collected along the Purros-Sesfontein-Kamanjab profile showed two groupings of mineral ages: (1) a grouping at ∼490 Ma interpreted as cooling following a tectono-thermal event at ∼530 Ma; and (2) a grouping at ∼ 460 Ma that was not related to any metamorphic event (Ahrendt et al., 1983b). K/Ar biotite data from the Southern Kaoko Belt (Ugab Domain) were interpreted as cooling ages following a regional metamorphic event at ∼490 Ma (Ahrendt et al., 1983b; Porada et al., 1983; Weber et al., 1983).

Subsequently, U/Pb zircon and monazite dating of granitic plutons and orthogneisses indicate that Kaoko Belt transpressional orogenesis occurred between 580 and 550 Ma, with an older high-grade event at 655–645 Ma in the westernmost part (Seth et al., 1998, 2000; Franz et al., 1999; Kröner et al., 2004). Sm/Nd dating of garnets associated with peak metamorphic assemblages in the Central and Eastern Zones of the Kaoko Belt gave a uniform age of 576 ± 15 Ma (Goscombe et al., 2003b).

Most recently, zircon and monazite U/Pb dates, garnet Sm/Nd dates and hornblende $^{40}Ar/^{39}Ar$ dates throughout the Kaoko Belt helped define three distinct tectono-metamorphic events (Goscombe et al., 2005b); an older M1 (655–645 Ma) high-grade event restricted to the westernmost Coastal terrane, a high-grade M2 (580–550 Ma) transpressional phase, and a younger, lower-grade M3 (535–505 Ma) phase of NNE-SSW shortening related to deformation within the Damara Belt. Peak metamorphic assemblages and voluminous granitoid emplacement occurred in the highest-grade parts of the Kaoko Belt at 580–570 Ma (Goscombe et al., 2005b). Data from pegmatite dikes that cross cut the regional shear zones gave ages that indicate transpression deformation ended by 530–508 Ma.

3.3. Gariep Belt thermochronology

$^{40}Ar/^{39}Ar$ geochronology/thermochronology for the Gariep Belt (Frimmel and Frank, 1998) shows:

(1) Three groupings of hornblende $^{40}Ar/^{39}Ar$ ages within the Chameis Complex; a grouping at 600–630 Ma inferred to record the timing of high-T hydrothermal sea-floor alteration; a grouping between 576 and 573 Ma linked to subduction-related metamorphism as part of outboard accretionary prism development; and a grouping at 547–543 Ma considered to date peak metamorphism in the Marmora Terrane, and probable emplacement above the Port Nolloth Zone (see Fig. 2b).
(2) Syn-tectonic muscovite ages of 483 and 506–495 Ma for the northern and southern deformed platform and basement of the Port Nolloth Zone possibly record deformation post-Nama foreland basin deposition. This is supported by a whole-rock $^{40}Ar/^{39}Ar$ age of 496 ± 2 Ma from phyllite that constrains the timing of northeast-vergent folding and thrusting within the western part of the Nama foreland basin sequence (Gresse et al., 1988).

4. $^{40}Ar/^{39}Ar$ step-heating experiments

In this study $^{40}Ar/^{39}Ar$ geochronology was used to date muscovite and biotite separated selectively from different foliations and structural levels in the schist pile, and from overprinting high strain zones. Cleavage zones were also dated using carefully selected, cut, sub-mm sized whole rock fragments of cleavage mica in the low-grade outer flanks, because of the very fine grain size of the white micas (e.g., Foster et al., 1998, 1999). We also present data from a smaller number of hornblende separates.

4.1. Results

A summary of the samples analyzed, calculated ages and comments on the interpretation of the data are given in Table 1. The $^{40}Ar/^{39}Ar$ isotopic data and analytical methods are included in Appendix A. Age spectra diagrams for individual samples are given in Appendices 2A and 2B in Supplementary data and typical age spectra are grouped with respect to tectonic belts and internal structural zones (see Figs. 6 and 7).

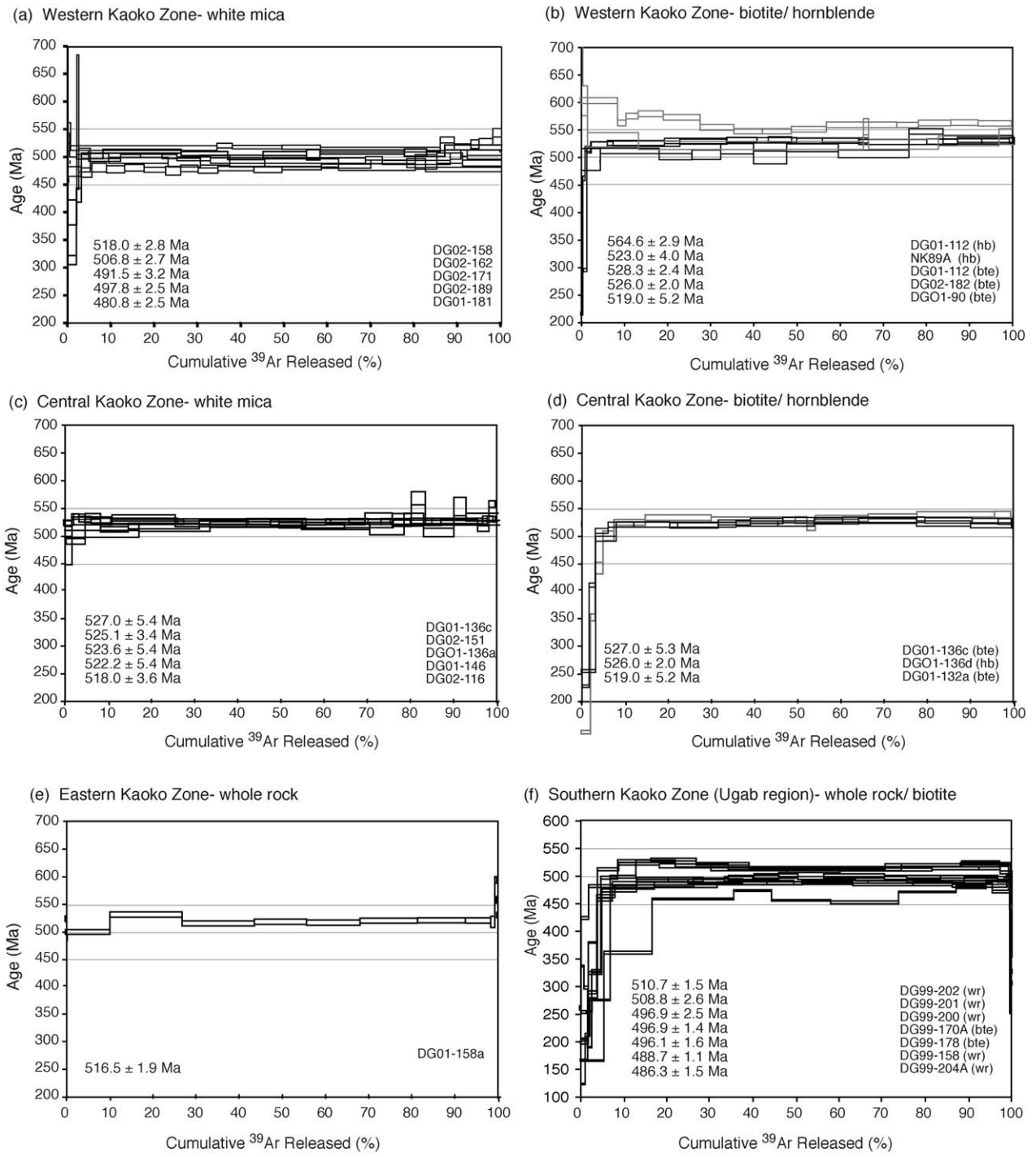

Fig. 6. Stacked $^{40}Ar/^{39}Ar$ age spectra for the Kaoko Belt. (a and b) Spectra from the Orogen Core of the Western Kaoko Zone. (c and d) Spectra from the Central Kaoko Zone. (e) Spectra from the Eastern Kaoko Zone. (f) Spectra from the Ugab Domain of the Southern Kaoko Belt. Samples numbers are shown on the right and the corresponding $^{40}Ar/^{39}Ar$ ages are listed (see Table 1 for details of the calculated ages).

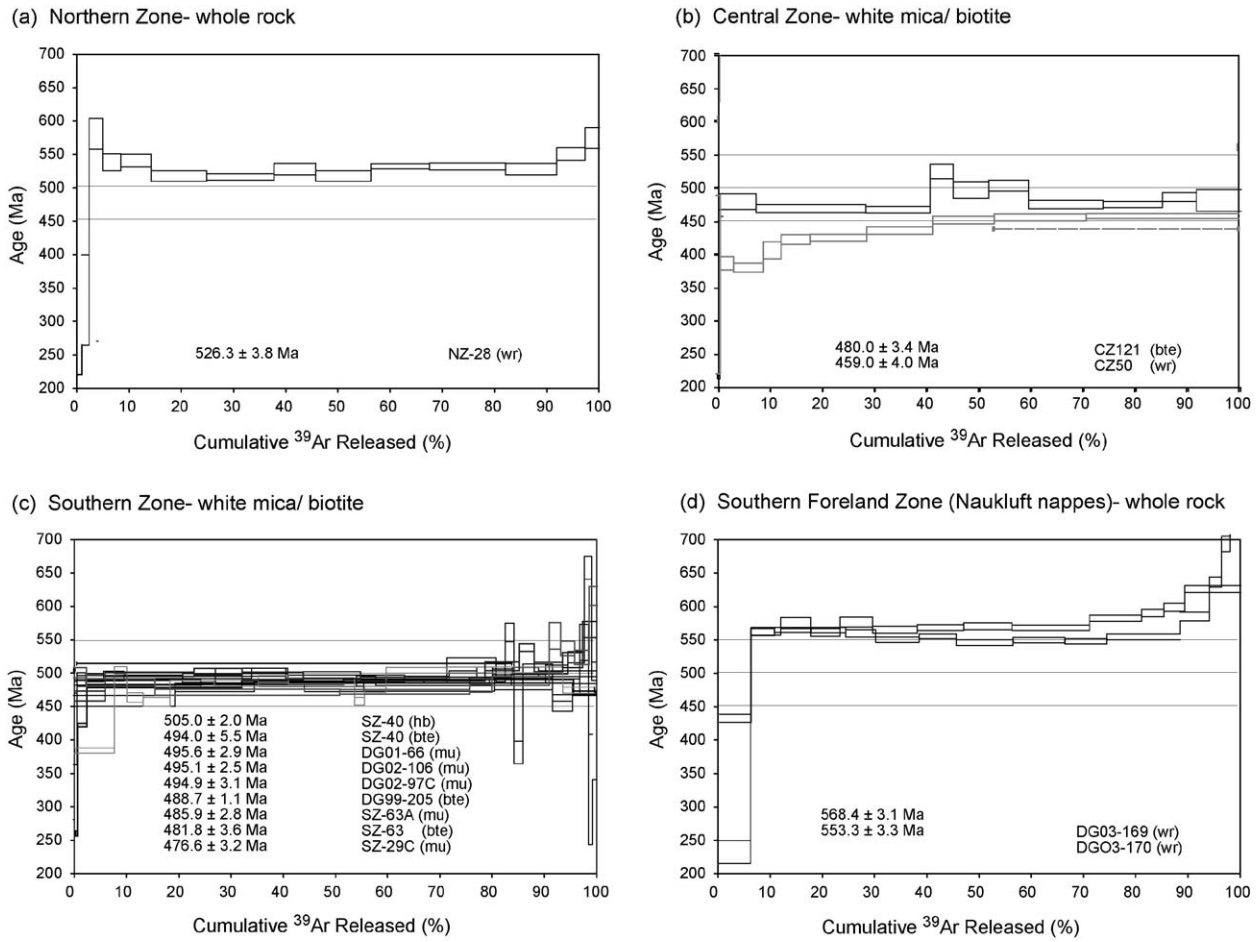

Fig. 7. Stacked $^{40}Ar/^{39}Ar$ spectra for the Damara Belt. (a) Whole rock $^{40}Ar/^{39}Ar$ step-heating experiment from the Northern Zone. (b) Spectra from the Central Zone. (c) Spectra from the Southern Zone, and (d) whole rock $^{40}Ar/^{39}Ar$ step-heating experiment from the Southern Foreland Zone. Samples numbers are shown on the right and the corresponding apparent ages are listed (see Table 1 for details of the calculated ages).

4.1.1. Kaoko Belt $^{40}Ar/^{39}Ar$ results

$^{40}Ar/^{39}Ar$ apparent age data are limited to the Western Kaoko Zone east of the Three Palms Mylonite Zone and to the Central Kaoko Zone (Figs. 2 and 4). There are no data presented in this study from the westernmost Coastal terrane due to sand cover and difficult access, related to the presence of lions and quick sand conditions in the Hoanib, Hoarusib and Khumib rivers, as well as drifting sand in the northern Sechomb, Ondondo and Nadas rivers (Fig. 4).

$^{40}Ar/^{39}Ar$ data for the Western Kaoko Zone include six white mica apparent ages of 518 ± 3 through 481 ± 3 Ma (Fig. 6a), four biotite apparent ages of 531 ± 5 Ma (KK50) through 519 ± 5 Ma (Fig. 6b) and three hornblende apparent ages 564 ± 3 Ma (KK86), 533 ± 4 Ma (NK79) and 527 ± 4 Ma (NK89) (Table 1 and Fig. 6b). White mica samples from near or within shear zones give younger apparent ages, particularly those from a mylonitised granite (NK71, Fig. 4) with an apparent age of 492 ± 3 Ma and a mylonitic orthogneiss (NK82, Fig. 4) with an apparent age of 481 ± 3 Ma.

Eight $^{40}Ar/^{39}Ar$ age spectra from samples from the Central Kaoko Zone gave a relatively tight population of apparent ages spanning only 8–10 m.y. for white mica, biotite and hornblende, which for white mica and biotite range from 527 ± 5 Ma (KK130, Fig. 4) and 518 ± 4 Ma (NK9, Fig. 4) (see Table 1 and Fig. 6c), 527 ± 5 Ma (KK130, Fig. 4) and 519 ± 5 Ma (KK126, Fig. 4) (see Table 1 and Fig. 6d), respectively, and a hornblende analysis gives 526 ± 2 Ma (KK130, Fig. 4) (see Table 1 and Fig. 6d). A sample of mylonitised fine-grained schist close to the Purros Mylonite Zone near Red Drum (NK96, Fig. 4) gives a much younger whole rock apparent age of 467 ± 3 Ma (Table 1).

Due to the low-metamorphic grade of the Eastern Kaoko Zone there is only one sample, a phyl-

litic slate from outcrops near Khowarib, east of Sesfontein (KK158a, Fig. 4) that gave an apparent age of 517 ± 4 Ma (Fig. 6e).

4.1.2. Ugab Domain-Northern Zone $^{40}Ar/^{39}Ar$ results

Samples from the Southern Kaoko Zone (Ugab Domain) are from chevron-folded turbidites cropping out on and near the Ugab River, a region bounded by the Ogden Mylonite Zone on the west, the Etendeka Basalts on the northwest, the Omangambo Granite on the east and the Brandberg/Messum Volcanic Complexes in the south (Fig. 5). These give $^{40}Ar/^{39}Ar$ ages of (1) 511–509 Ma (samples DG99-201 and DG99-202, Fig. 6f), 497–496 Ma (samples DG99-200, DG99-178 and DG99-170A, Fig. 6f), as well as more discordant spectra near granitic plutons that give apparent ages of 486 ± 3, 480 ± 4 and 438 ± 2 Ma (samples DG99-158, DG99-170 and DG99-204, Fig. 5) (also see Table 1).

The oldest apparent ages come from fine-grained phyllitic slates furthest away from the Voetspoor, Doros and Omangambo Granites (Fig. 5). Samples closer to the granites are in general coarser grained, have more typical "schist or hornfels like" fabrics with visible biotite flakes, and have more discordant spectra (Fig. 6f). These are from within granite contact aureoles.

4.1.3. Damara Belt $^{40}Ar/^{39}Ar$ results

Northern and Central Zone data are limited (Figs. 2, 5 and 8), but a whole rock $^{40}Ar/^{39}Ar$ age of 526 ± 4 Ma (Fig. 7a) was obtained from a slate near Summas in the Northern Zone (NZ28, Fig. 5) and white mica and biotite separates from Central Zone schists and migmatites (samples CZ 121 and CZ50, Fig. 8) gave 480 ± 3 and 459 ± 4 Ma apparent ages (Fig. 7b).

Nine schist samples from the Southern Zone of the Damara Belt (Fig. 8) gave white mica $^{40}Ar/^{39}Ar$ ages of ∼495 Ma (samples DG01-66, DG02-106 and DG02-97C, Fig. 7c), and biotite apparent ages of 494 ± 6 and 489 ± 1 Ma (samples SZ40 and DG99-205, Fig. 7c). Samples in close proximity to the Donkerhuk Granite show thermal resetting and discordance with apparent ages of 486 ± 3, 482 ± 4 and 477 ± 3 Ma (samples SZ63A, SZ63 and SZ29C, Fig. 7c).

Samples of a phyllitic slate (DG03-169, Fig. 8) and a phyllite (DG03-170, Fig. 8) gave $^{40}Ar/^{39}Ar$ ages of 568 ± 3 and 553 ± 3 Ma, respectively (Fig. 7d) from the Naukluft Nappes of the Southern Foreland (Figs. 2 and 8). These spectra show discordance related to the presence of a residual non-recrystallized detrital mica component (see Fig. 7d).

5. Discussion

The Kaoko, Gariep and Damara Belts show separate and distinct deformational, metamorphic and cooling histories recorded by individual $^{40}Ar/^{39}Ar$ samples (Fig. 9).

The Kaoko Belt shows some internal complexity, but the majority of the $^{40}Ar/^{39}Ar$ white mica and biotite apparent ages fall between 530 and 510 Ma. The Orogen Core of the Western Kaoko Zone (Fig. 9) shows the greatest apparent age variability, with possible influences from the continued activity and mica growth along the major shear zones as well as marked metamorphic grade variations documented by Goscombe et al. (2005a). The Central Kaoko Zone (Fig. 9) shows more uniformity in $^{40}Ar/^{39}Ar$ apparent age data (527–518 Ma), which overlaps a phyllite-whole rock apparent $^{40}Ar/^{39}Ar$ age of ∼517 Ma from the low-grade Eastern Kaoko Zone. In the Central Kaoko Zone hornblende, biotite, and muscovite from location KK130 all give concordant ages at ∼524–527 Ma, which indicates very rapid cooling from above 550° to below 300 °C in less than ∼3 m.y. (about 50–100 °C/m.y.). The youngest ages (∼510 Ma) are in the Ugab region of the Southern Kaoko Belt (Fig. 9). Thermal effects from the Voetspoor, Doros and Omangambo Granites cause resetting and discordance in $^{40}Ar/^{39}Ar$ spectra with apparent ages generally from 500 to 480 Ma (Fig. 9).

The Damara Belt $^{40}Ar/^{39}Ar$ data show a distinct age zonation related to the granite-dominated Central Zone, the transposed schist of the Southern Zone and the Northern and Southern marginal fold-thrust Zones (Figs. 8 and 9). The youngest ages come from the Central Zone where granite intrusion significantly influenced the thermal regime, and caused partial argon loss from the micas in the host metamorphic rocks; $^{40}Ar/^{39}Ar$ muscovite and biotite apparent ages are ∼480 and ∼460 Ma, respectively (Fig. 9). In the Southern Zone the $^{40}Ar/^{39}Ar$ muscovite and biotite apparent ages are tightly grouped at ∼495–494 Ma, with local effects from the late, post-tectonic Donkerhuk granite which resulted in argon loss as detected by disturbed age spectra and apparent ages as young as ∼477 Ma (Fig. 9).

The oldest $^{40}Ar/^{39}Ar$ ages come from whole-rock analyses of cleavage mica from the low-grade flanks and these are ∼526 Ma for the Northern Zone, and 553 and 568 Ma for the Naukluft Nappes of the Southern Foreland (Fig. 9). These results are broadly concordant with the less precise published K/Ar ages for both these zones. K/Ar ages in the North Pavian Thrust sheet of the Naukluft Nappes (see Fig. 12 of Weber et al., 1983) are 547 ± 17 and 532 ± 16 Ma (samples Nau 3 and 11

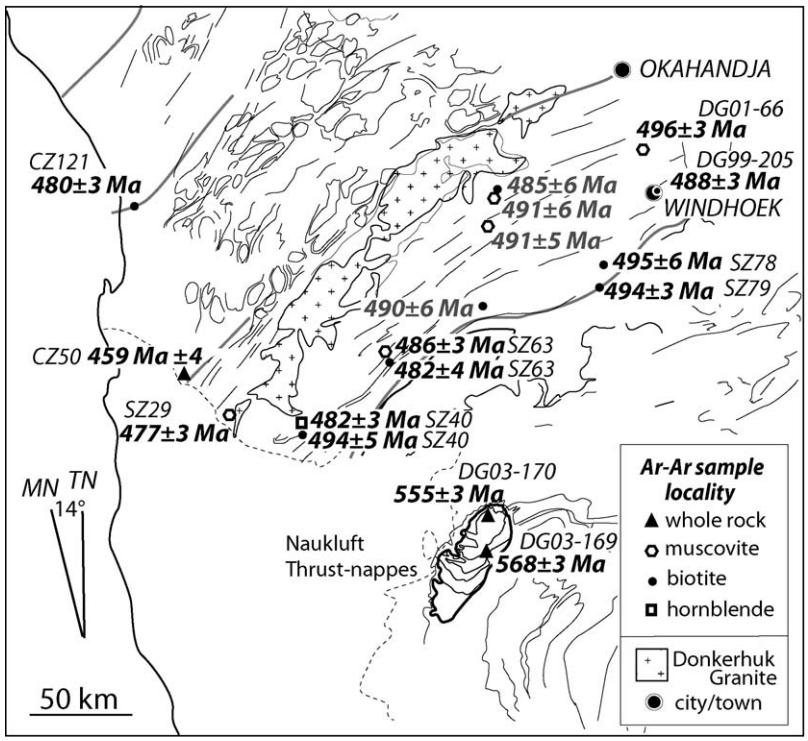

Fig. 8. $^{40}Ar/^{39}Ar$ data plotted on a formline structural map of the Central, Southern and Southern Margin Zones and Southern Foreland of the Damara Belt. See Fig. 1 for location. Includes data from Kukla (1993) in grey scale.

from Remhoogte Farm listed in Table 3, Ahrendt et al., 1977). An $^{40}Ar/^{39}Ar$ whole rock analysis from a silver-grey phyllite from the same thrust sheet close to these localities give a plateau age of 553 ± 3 Ma (DG03-170, Fig. 7d). The $^{40}Ar/^{39}Ar$ age for DG03-169 (Fig. 7d) of 568 ± 3 Ma is also from the North Pavian Thrust sheet, but south of the Remhoogte Farm localities in the Tsondab River Valley near Blässkranz Farm (see map sheet of Korn and Martin, 1959).

These cleavage ages are interpreted to be metamorphic crystallization ages as illite crystallinity data suggest that this part of the Naukluft Nappes did not attain temperatures above 350 °C (Ahrendt et al., 1977, p. 739), and therefore were below the argon closure temperature for white mica. The age spectra, however, for these samples are partly discordant in the higher temperature steps indicative of the presence of a partly degassed detrital mica component (see Fig. 7d). Ahrendt et al. (1977, pp. 738–739) defined two white mica K/Ar isochron ages for the folded Nama beds and Klein Aub Formation immediately underlying the Naukluft Nappes; ages of 530 ± 10 Ma, which they considered the age of metamorphism and therefore deformation, and 495 ± 10 Ma, which they considered as a possible cooling age but could not discount possible rejuvenation by deformation during nappe emplacement. Similar 495 Ma ages were found in the highest thrust sheets of the Naukluft Thrust stack, and these samples contained biotite (Ahrendt et al., 1977; Fig. 12 of Weber et al., 1983).

5.1. Implications for Damara Orogen tectonothermal evolution

Integration of these new $^{40}Ar/^{39}Ar$ thermochronologic data (Fig. 9) with published U-Pb zircon, monazite and titanite geochronology data in time-space diagrams (Fig. 10) provides a better definition of the peak metamorphic and cooling history for the different parts of the Damara Orogen (Fig. 11). Major periods of cooling follow peak metamorphism in the different structural and tectonic zones by some 20–30 m.y. Cooling through the temperature interval of about 550–300 °C is different in the different zones, occurring at about 535–510 Ma in the Kaoko Belt proper, about 510–480 Ma in the Southern Kaoko Belt, about 480–455 Ma in the Central Zone of the Damara Belt, about 500–485 Ma in the Southern Zone of the Damara Belt and about 535–525 Ma in the Gariep Belt (Fig. 11).

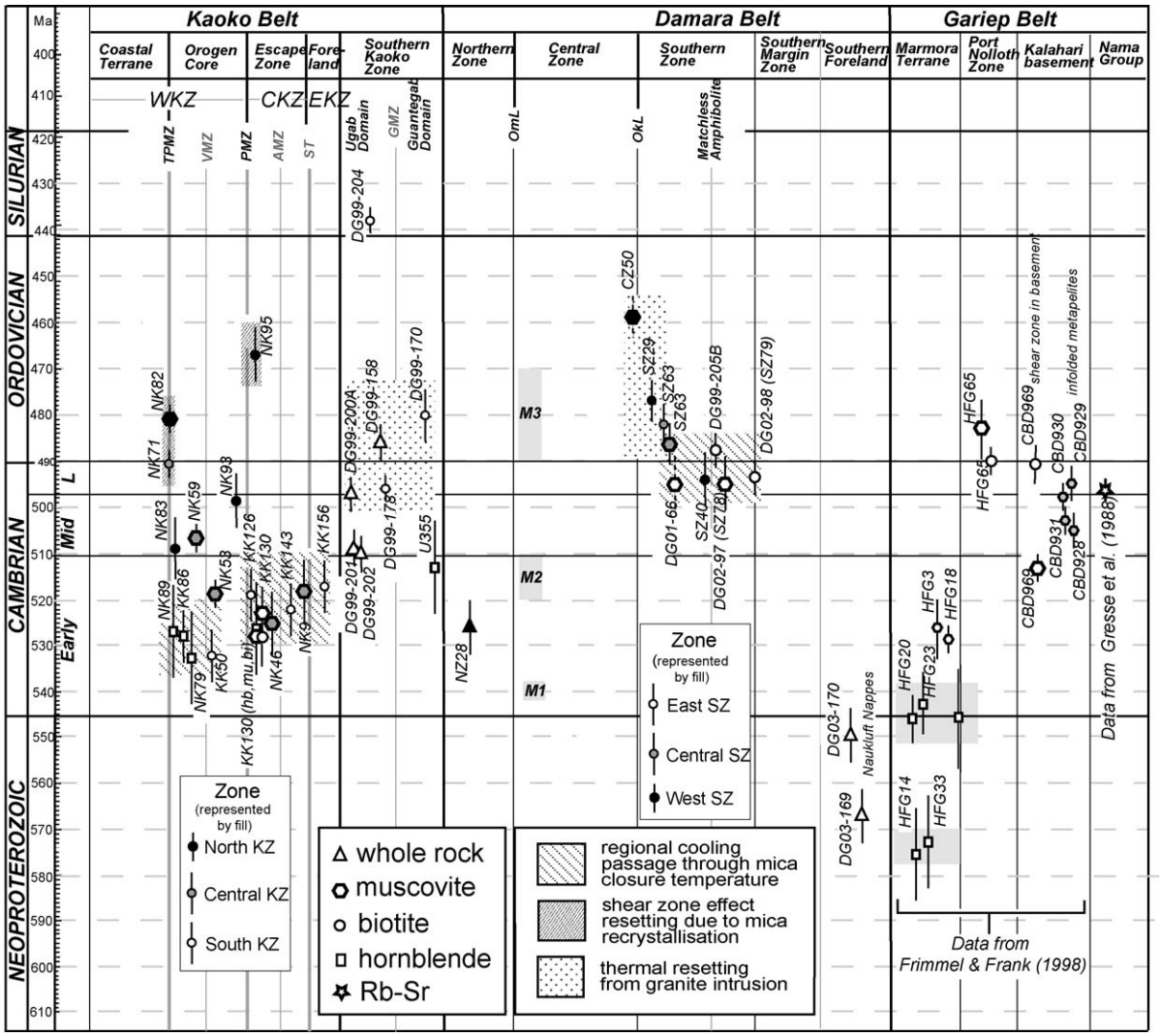

Fig. 9. Damara Orogen time-space plot of the $^{40}Ar/^{39}Ar$ data from this paper plotted for the Kaoko and Damara Belts, along with published data from Frimmel and Frank (1998) for the Gariep Belt. Effects from regional cooling through the mineral closure temperature (dotted oblique slashed lines), dynamic recrystallization in shear zones (close spaced oblique slashed lines), and thermal resetting from granites (stipple) are superimposed onto the $^{40}Ar/^{39}Ar$ data to illustrate the significance of these data. WKZ: Western Kaoko Zone; CKZ: Central Kaoko Zone; EKZ: Eastern Kaoko Zone; TPMZ: Three Palms Mylonite Zone; VMZ: Village Mylonite Zone; PMZ: Purros Mylonite Zone; AMZ: Ahub Mylonite Zone; ST: Sesfontein Thrust; GMZ: Guantegab Mylonite Zone; OmL: Omaruru Lineament (Shear Zone); OkL: Okahandja Lineament (Shear Zone).

In the Kaoko Belt, the Orogen Core of the Western Kaoko Zone (see Fig. 11) underwent peak metamorphism (800–850 °C and 7–9 kbar) at 580–560 Ma, with passage through 550–500 °C at 535–528 Ma and 350–300 °C at 525–505 Ma, with a spatially restricted thermal pulse at ~508–505 Ma associated with post-kinematic pegmatite swarms (Goscombe et al., 2005b). The Central Kaoko Zone experienced peak metamorphic conditions in the west of 700 °C and 7–9 kbar at ~575 Ma (Fig. 11). Hornblende and mica $^{40}Ar/^{39}Ar$ from this belt give similar ages (Table 1) indicating relatively rapid cooling (rates up to 50–100 °C/m.y.) of the zone through about 550–300 °C between 528 and 518 Ma.

The thermal history of the Damara Belt peaked at ~750–700 °C and ~5 kbar (Jung and Mezger, 2003) during intrusion of the granitic plutons of the Northern and Central Zones (compare Figs. 10 and 11). Regional cooling through 350–300 °C occurred in the Central Zone from 490 to 460 Ma, immediately after the emplacement of the post-tectonic A-type granites, despite distinct pulses of magmatism at 570–540, 535–510 and

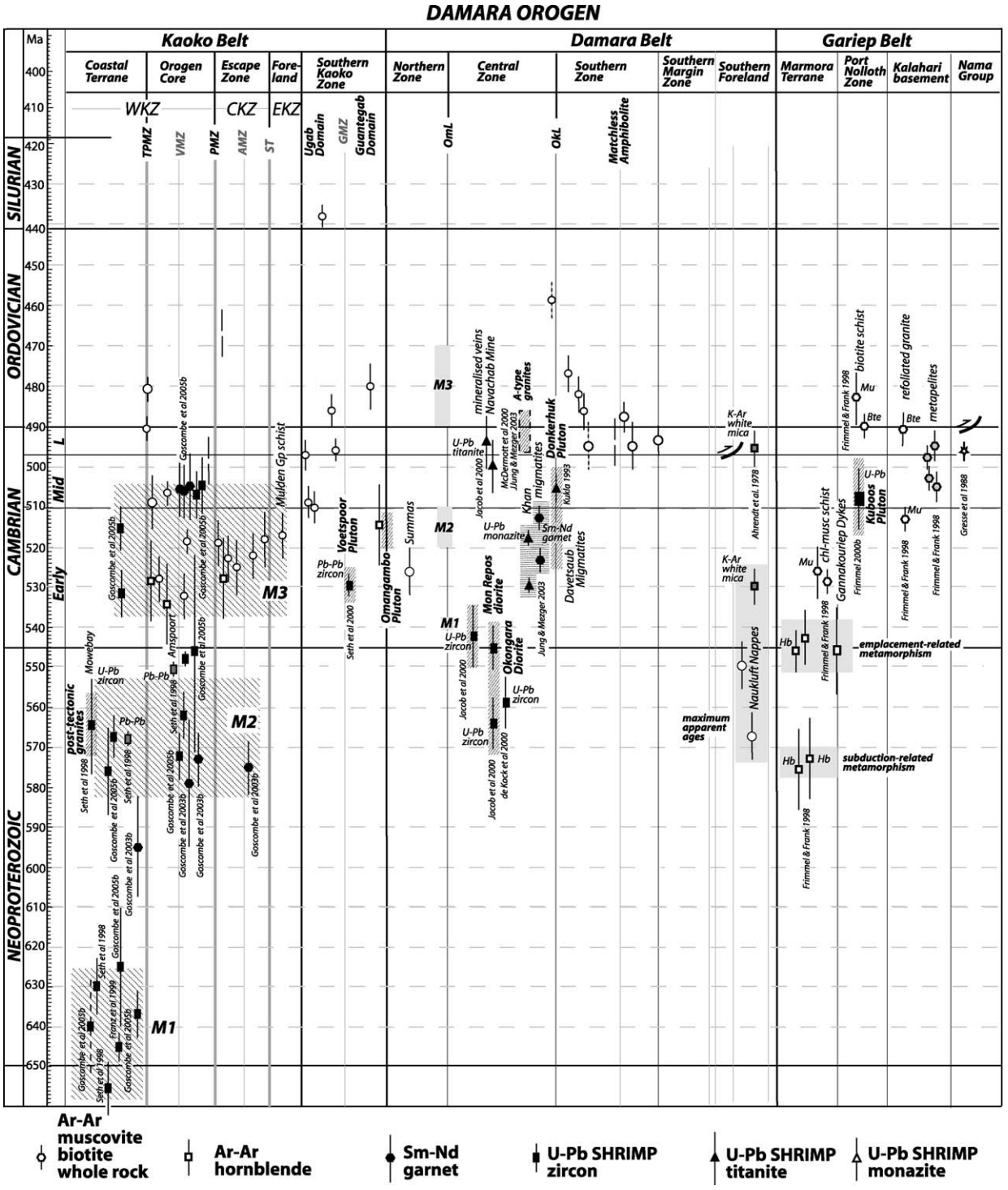

Fig. 10. Damara Orogen time-space plot of the recently published geochronological data including the $^{40}Ar/^{39}Ar$ data from Fig. 9, and U-Pb data on zircon, monazite and titanite. Sources are listed in the figure. Unsourced data is from this paper. Fault and shear zone abbreviations are as listed in Fig. 9 caption (Frimmel, 2000b).

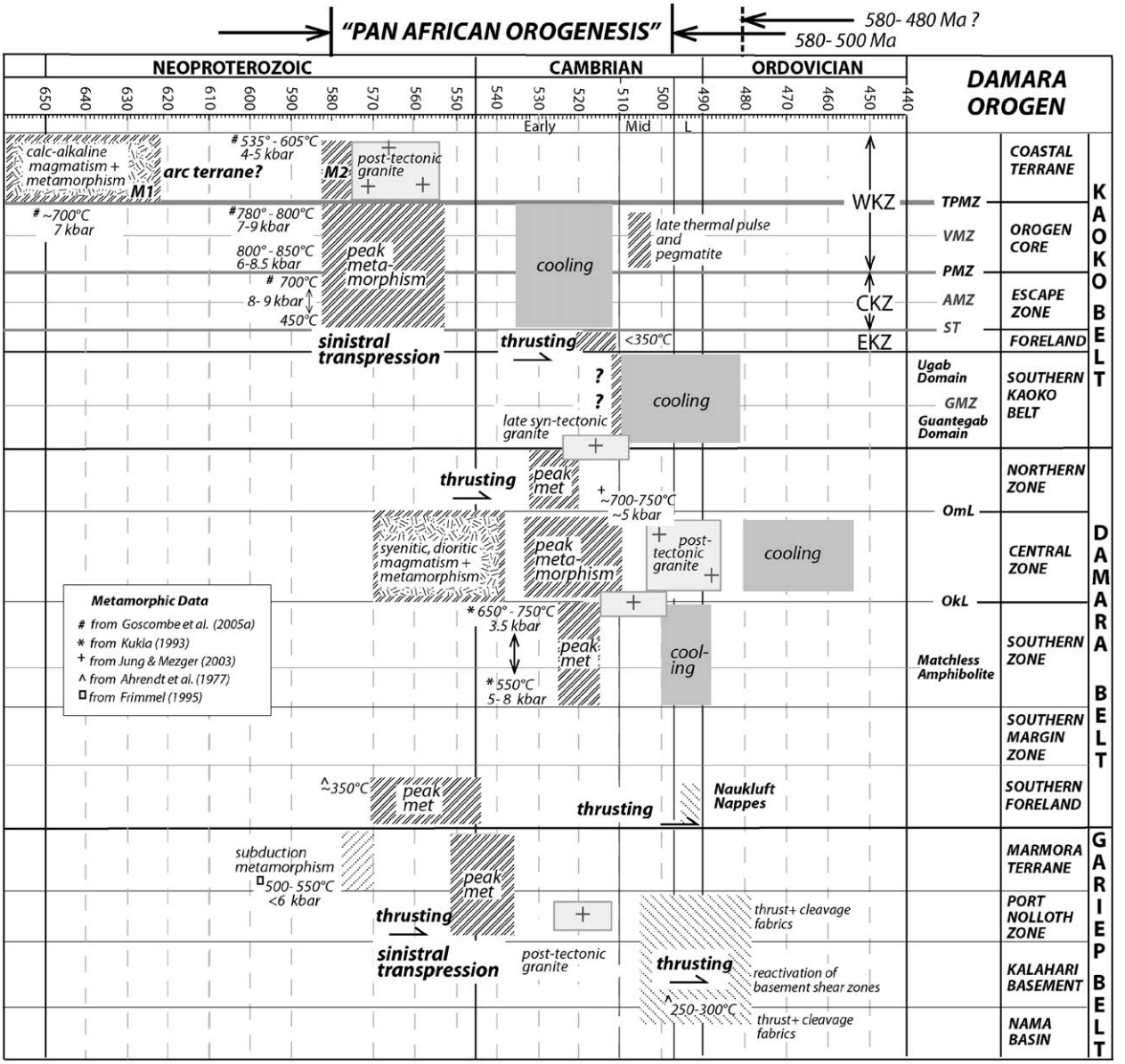

Fig. 11. Summary time-space diagram for the Damara Orogen based on the data presented in Figs. 9 and 10. The plot encapsulates the complexity of magmatic, metamorphic, deformational and cooling patterns across the orogen (see Fig. 12) as part of Pan-African orogenesis. Fault and shear zone abbreviations are as listed in Fig. 9 caption.

505–485 Ma (Figs. 10 and 11). This cooling history contrasts with that of the Southern Zone poly-deformed and transposed schists that have a distinct clustering of biotite and white mica apparent cooling ages of 505–495 Ma. Data in this paper and data from Jung and Mezger (2003) suggest a more complicated pattern of deformation, metamorphism, magmatism and cooling across the Damara Belt (see Fig. 12a and b) than previous interpretations of slow cooling and uplift following a single metamorphic event at ~520 Ma (e.g., Haack and Hoffer, 1976; Haack et al., 1980).

5.2. Implications for Pan-African Orogeny

The new thermochronological data and review of the more recent, higher precision geochronological data presented here (Fig. 10) better constrain the timing of the tectonic events that make up the Pan-African orogeny in

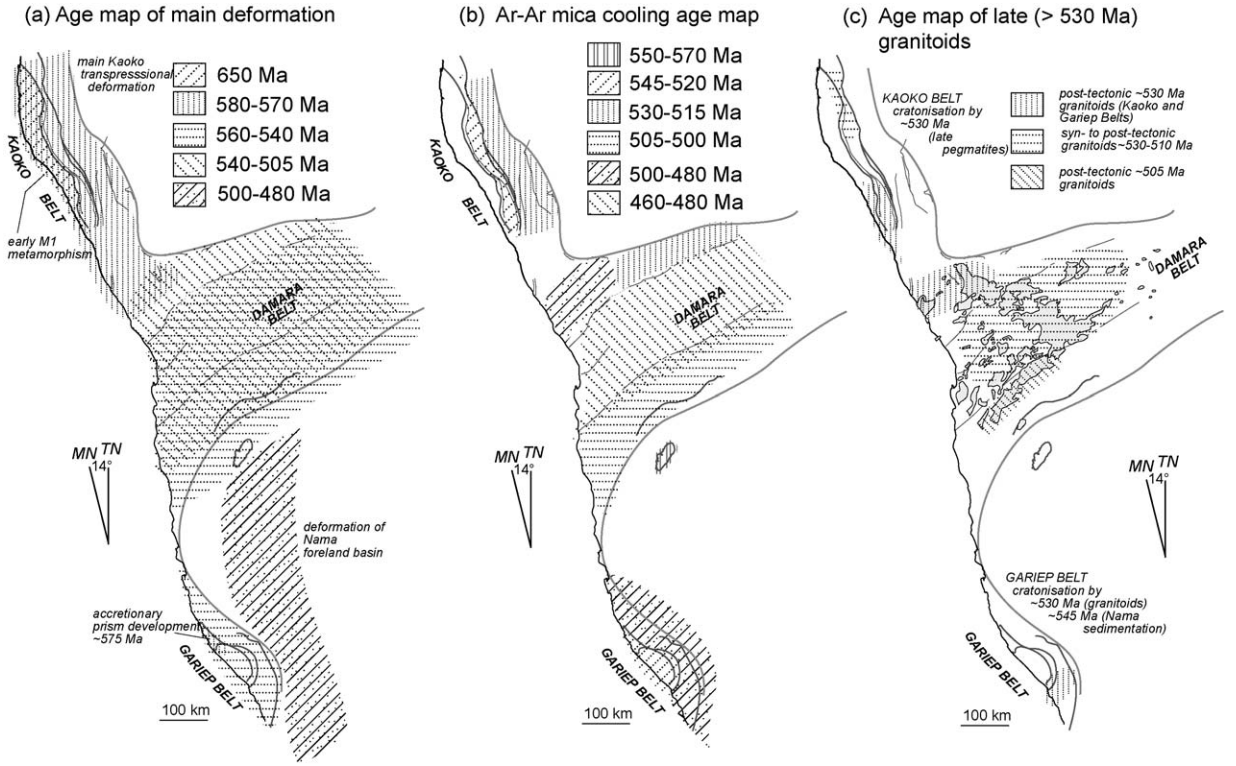

Fig. 12. Damara Orogen synoptic maps showing (a) age distribution map of the main deformation, (b) $^{40}Ar/^{39}Ar$ cooling age map, and (c) age map of the late (>530 Ma) granitoids. Data sources are shown on Fig. 10.

Namibia and that of continental welding in this part of Gondwana.

The Pan-African orogeny was originally defined at ~500 Ma (Kennedy, 1964), based on K/Ar and Rb/Sr mineral ages which record the late thermal history rather than the timing of peak deformation and metamorphism (Kröner, 1980, 1982). Since publication of the first cooling ages of Clifford (1967) and Haack and Hoffer (1976) there has been debate about the nature and duration of Pan-African orogenesis (e.g., Kröner and Clauer, 1979; Haack et al., 1980; Kröner, 1982). With more precise U/Pb SHRIMP zircon, monazite and titanite dating (e.g., Franz et al., 1999; Jung and Mezger, 2003; Goscombe et al., 2005b) the concept of Pan-African orogenesis has evolved to a series of deformational and metamorphic events between 580 and 480 Ma (Fig. 11) (see also Hanson, 2003), with the final deformation expressed as basement shear zone reactivation in the Kalahari craton ~510–480 Ma (Frimmel and Frank, 1998).

5.3. A revised tectonic evolution of the Damara Orogen

This study along with other recent geochronological studies suggest that initiation of deformation and ocean closure for the Damara Belt occurred significantly earlier than considered previously. The metamorphic crystallization ages within the low-grade southern flank of the Damara Belt suggest that crustal thickening within a tectonic wedge, attendant with metamorphism, folding and cleavage development, may have been occurring at 570–550 Ma along the southern margin (Fig. 11). This was coincident with mafic magmatism and intrusion of diorites and syenites in the Central Zone from ~570–540 Ma (Jacob et al., 2000; de Kock et al., 2000), as well as sinistral transpressional deformation and metamorphism in the Kaoko Belt (Goscombe et al., 2003a, 2005b), and subduction related metamorphism at ~575 Ma followed by emplacement- or obduction-related metamorphism and sinistral transpression at ~550–540 Ma in the Gariep Belt (Frimmel and Frank, 1998).

A revised tectonic evolution is presented as a series of schematic non-palinspastic maps involving the Namibian part of the Damara Orogen (Fig. 13). The maps show the relationships between the various continental fragments including sedimentation, deformation, metamorphism and magmatism over the time interval from 780 to 480 Ma. The major tectonic intervals are discussed below.

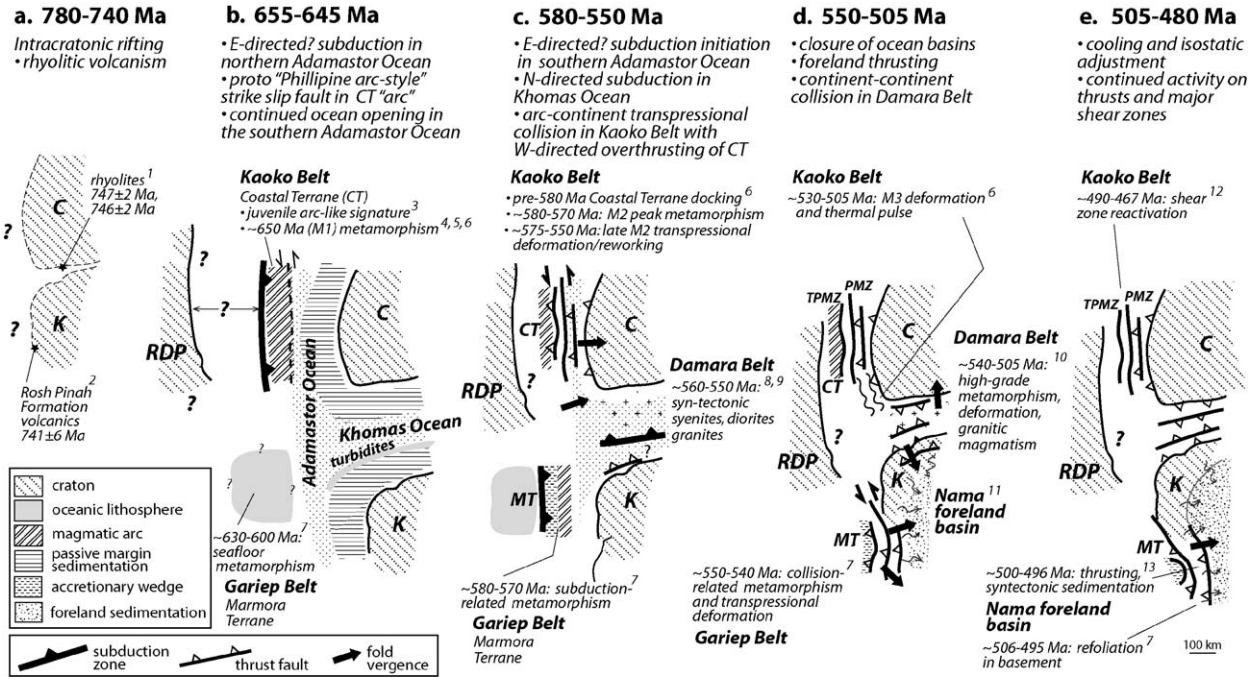

Fig. 13. Schematic 2D plate reconstructions for various time periods involving the Congo (C), Kalahari (K) and Rio de la Plata (RDP) cratons constrained by new and recent geochronologic and thermochronologic datasets. The positions and sizes of the intervening ocean basins between these cratonic fragments are poorly understood, as well as the links between the various inferred plate boundaries (e.g., subduction zones, transforms, etc.). Reconstruction of ocean closure is based on deformation kinematics related to stretching lineations, shear bands and fold- and fault relationships. Constraints from the South America side are not included and therefore not shown in the figure. Timing constraints include (1) Hoffman et al. (1996); (2) Frimmel et al. (1996); (3) Masberg et al. (2005); (4) Franz et al. (1999); (5) Seth et al. (1998); (6) Goscombe et al. (2005a,b); 7: Frimmel and Frank (1998); (8) Jacob et al. (2000); (9) de Kock et al. (2000); (10) Jung and Mezger (2003); (11) Gresse and Germs (1993); (12) this paper; (13) Gresse et al. (1988). MT: Marmora Terrane (Gariep Belt); TPMZ: Three Palms Mylonite Zone (Kaoko Belt); PMZ: Purros Mylonite Zone (Kaoko Belt).

5.3.1. Intracratonic rifting: 780–740 Ma (Fig. 13a)

Continental breakup and intracratonic rifting, as evidenced by rhyolitic volcanism, was well under way by ~750 Ma (Frimmel et al., 1996; Hoffman et al., 1996), although the positions of the Congo, Kalahari and Rio de la Plata cratons may be quite disparate at about 750 Ma; see Fig. 2 of Collins and Pisarevsky (2005) for an example of a recent reconstruction.

Development of the Adamastor and Khomas Oceans most likely continued through 600 Ma (see Section 5.3.2), although the size or dimensions of the Khomas Ocean basin have been disputed (see Kröner, 1977; Porada, 1989). Suggested sources for the detritus in Damara turbidites within these ocean basins is presented in Fig. 17 of Goscombe et al. (2005b).

5.3.2. Subduction in northern Adamastor Ocean with continued spreading and passive margin sedimentation elsewhere: 655–645 Ma (Fig. 13b)

Ocean closure initiated in the northern Adamastor Ocean at the level of the Kaoko Belt by about 655 Ma, as suggested by an older ~650 Ma high-T metamorphism (Seth et al., 1998; Franz et al., 1999; Goscombe et al., 2005a,b) and arc-like magmatic signatures (Masberg et al., 2005) within the Coastal Terrane of the Kaoko Belt. W-directed subduction has been inferred from the presence of the arc (Masberg et al., 2005) but the lack of any suture and/or high-P metamorphic relicts inboard of the Coastal Terrane (cf. Konopásek et al., 2004; Goscombe et al., 2005a,b) may reflect former E-directed subduction.

Continued spreading in the southern Adamastor Ocean is supported by relicts of seafloor metamorphism in ophiolitic fragments from the Marmora Terrane (Frimmel, 1995; Frimmel and Frank, 1998).

5.3.3. Docking of arc (Coastal Terrane) in the Kaoko Belt and subduction initiation in southern Adamastor Ocean and Khomas Ocean: 580–550 Ma (Fig. 13c)

Docking of the "exotic" western-most Coastal Terrane by 580 Ma (Goscombe et al., 2005b) appears asso-

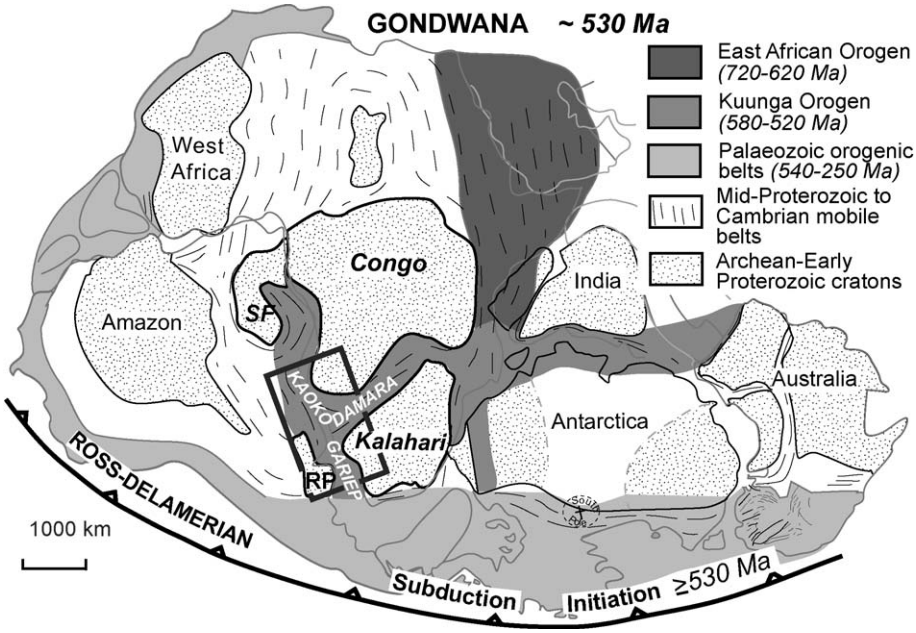

Fig. 14. Map of the Gondwana supercontinent at the end of Neoproterozoic and beginning of Cambrian time (modified from Foster and Gray, 2000), showing the extent of the Kuunga Orogeny, the earlier East African Orogeny, and the continental margin Ross-Delamerian Orogeny (modified from Meert, 2003). The heavy lined rectangle indicates the region depicted in Fig. 13d. SF: Sao Frisco Craton; RP: Rio de La Plata craton.

ciated with peak metamorphism and the main transpressional phase of deformation in the Kaoko Belt from ~575 to 550 Ma (Goscombe et al., 2005b). This clearly predates final basin closure in either the Gariep or the Damara Belts, at 550–540 and 510–495 Ma, respectively, despite continued activity along the major Kaoko Belt shear zones through ~470 Ma (Fig. 9).

Sinistral transpressive deformation of the Kaoko Belt may have been diachronous, migrating southwards. This is suggested by the apparent younger $^{40}Ar/^{39}Ar$ ages in the Ugab region, at the junction of the N-trending Kaoko Belt with the ENE-trending Damara Belt, although interpretation of the $^{40}Ar/^{39}Ar$ spectra may be more complicated due to intrusion of the Voetspoor, Doros and Omangambo Granites.

5.3.4. Crustal thickening phase with final closure of the Adamastor and Khomas Oceans: 550–505 Ma (Fig. 13d)

Crustal thickening and metamorphism along the northern or Congo cratonic margin of the former Khomas Ocean basin, Damara Belt (Goscombe et al., 2004) was occurring at ~525 Ma (this paper) suggestive of diachronous deformation across the Damara Belt with asymmetric ocean closure due to N-directed subduction of the Khomas Ocean lithosphere and overlying Kuiseb turbidites beneath the leading edge of the attenuated Congo craton (cf. Barnes and Sawyer, 1980; Kasch, 1983b). Deformation migrated southwards initially and then expanded northwards, marked finally by both north-directed thrusting across the Congo craton (Kamanjab Inlier) and coupled south- (Damara Belt) and east-directed (Gariep Belt) overthrusting onto the Kalahari craton from ~495 to ~480 Ma (Gresse et al., 1988; Germs and Gresse, 1991; Gresse and Germs, 1993). This final phase was contemporaneous with closure of the southern Adamastor Ocean due to inferred W-directed subduction of the Kalahari craton (see Fig. 7 of Frimmel and Frank, 1998), although E-directed subduction is now favoured by Basei et al. (2005) based on sediment provenance data. Pulses of magmatism and high-T/low-P metamorphism continued in the Central Zone from 540 to 510 Ma (Jung and Mezger, 2003).

Late stage, E-directed, semi-brittle thrusting of the Kaoko Belt across the Congo craton was underway by ~516 Ma (this paper) with broad warpings of the earlier-formed Kaoko Belt transpressional structures related to a component of N–S shortening in the period 530–495 Ma (M3 shortening of Goscombe et al., 2005b). There may have also been periods of extension and transtensional deformation, regionally and along the major structures, respectively, in the Kaoko Belt, giving rise to rapid cooling and exhumation in the Central Kaoko Zone.

Closure of the Khomas Ocean by about 540–520 Ma coincided with intense and widespread Kuunga Orogeny that united Gondwana by about 530 Ma (e.g., Meert, 2003; Boger and Miller, 2004) (Fig. 14). Subduction under Gondwana and began as early as about 560 Ma off of Antarctica, but was well established by about 530 Ma from Australia through South America. Major arc collisions and magmatism in the Ross-Delamerian orogeny took place by 520–510 Ma (e.g., Goodge et al., 1993; Goodge, 1997; Meert, 2003; Boger and Miller, 2004; Foster et al., 2005). At the scale of Gondwana the later-stage metamorphic and deformational events in the Damara Orogen, therefore, took place in an intraplate setting.

5.3.5. *Post-tectonic magmatism, cooling and isostatic adjustment: 505–480 Ma (Fig. 13e)*

Crustal thickening attendant with final ocean closure and assembly of West Gondwana led to post-tectonic magmatism and localized extension. Post-Kuunga and Ross-Delamerian extension was widespread along the margins of Gondwana as well as within the major mobile belts (e.g., Meert, 2003; Foster et al., 2005; Foden et al., 2006). In the Damara Belt this is marked by intrusion of A-type granites (McDowell et al., 2000) and in the Kaoko Belt by late pegmatites (Goscombe et al., 2005b). The post-tectonic magmatism was followed by final cooling and stabilization of the Damara Orogen, but cooling is somewhat diachronous across the orogen (see Fig. 12b).

Acknowledgements

Support for the research was from an Australian Research Council (ARC) Large Grant A00103456 awarded to D.R.G. and National Science Foundation Grant EAR-0440188 to D.A.F. Data analysis and manuscript preparation was completed by D.R.G. as part of an Australian Professorial Research Fellowship supported on ARC Discovery Grant DP0210178 (awarded to D.R.G.). We thank Michael Hartley and James Vogl for assistance with the $^{40}Ar/^{39}Ar$ analyses at UF, and Terry Spell for access to the argon lab at UNLV. We also thank Dr. Gabbi Schneider (Director), Charlie Hoffmann (Deputy Director), Mimi Dunaiski and Thomas Bekker of the Namibian Geological Survey for support, Peter Weber (Bushveld Car Hire) for assistance with vehicles and Gordon Holm (The University of Melbourne) for thin section preparation. We acknowledge discussions on Namibian geology with Charlie Hoffmann, Roy Miller, and Paul Hoffman, and comments by Hartwig Frimmel and an anonymous reviewer that helped us improve the manuscript.

Appendix A

A.1. Analytical methods

$^{40}Ar/^{39}Ar$ analyses of the samples were undertaken at the University of Florida, and the University of Nevada Las Vegas, following standard methods (e.g., McDougall and Harrison, 1999). Samples analyzed at the University of Florida were irradiated in the core of the Oregon State University research reactor facility along with the flux monitor GA1550 biotite (98.8 Ma). Samples were heated in a double vacuum resistance furnace with a tantalum crucible, or with a 30 W CO_2 laser. Laser-step heating was done with a defocused beam by changing the power output of the laser. Gas was expanded into a stainless steel clean-up line and purified with two 50 l s^{-1} SAES getters. Argon isotopes were measured using a MAP215-50 mass spectrometer in electron multiplier mode. Data were corrected for system blanks, machine background, and mass discrimination as determined by analyzing atmospheric argon. Correction factors for interfering isotopes were determined by analyzing irradiated K-glass and optical grade CaF_2 salts. Data reduction was done using ArArCALC (Koppers, 2002).

Samples analyzed at the University of Nevada Las Vegas were wrapped in Sn foil and stacked in fused silica tubes with the neutron fluence monitor FC-2 (Fish Canyon Tuff sanidine). Samples were irradiated at the Ford reactor, University of Michigan for 6 h in the L67 position. Correction factors for interfering neutron reactions on K and Ca were determined by repeated analysis of K-glass and CaF_2 fragments included in the irradiation. Measured $(^{40}Ar/^{39}Ar)_K$ values were 1.56 $(\pm 38.21) \times 10^{-2}$. Ca correction factors were $(^{36}Ar/^{37}Ar)_{Ca} = 2.79$ $(\pm 6.09) \times 10^{-4}$ and $(^{39}Ar/^{37}Ar)_{Ca} = 6.61$ $(\pm 0.21) \times 10^{-4}$. Samples were heated using a double vacuum resistance furnace. Reactive gases were removed by two GP-50 SAES getters prior to expansion into a MAP 215-50 mass spectrometer. Peak intensities were measured using a Balzers electron multiplier. Mass spectrometer discrimination and sensitivity was monitored by repeated analysis of atmospheric argon aliquots from an on-line pipette system. The sensitivity of the mass spectrometer was 6×10^{-17} mol mV^{-1}. Line blanks averaged 17.33 mV for mass 40 and 0.06 mV for mass 36.

Appendix B. Supplementary data

Supplementary data associated with this article can be found, in the online version, at doi:10.1016/j.precamres.2006.07.003.

References

Ahrendt, H., Behr, H.-J., Clauer, N., Hunziker, J.C., Porada, H., Weber, K., 1983a. The northern branch: depositional development and timing of the structural and metamorphic evolution within the framework of the Damara Orogen. In: Martin, H., Eder, F.W. (Eds.), Intracontinental Fold Belts. Springer-Verlag, Berlin, pp. 723–743.

Ahrendt, H., Behr, H.-J., Clauer, N., Hunziker, J.C., Porada, H., Weber, K., 1983b. K-Ar age determinations from the Northern Damara Branch and their implications for the structural and metamorphic evolution of the Damara Orogen, South West Africa/Namibia. In: Miller, R.G. (Ed.), Evolution of the Damara Orogen of South West Africa/Namibia, vol. 11. Geological Society of South Africa Special Publication, pp. 299–306.

Ahrendt, H., Hunziker, J.C., Weber, K., 1977. Age and degree of metamorphism and time of nappe emplacement along the southern margin of the Damara Orogen/Namibia (SW-Africa). Geol. Rund. 67, 719–742.

Barnes, S., Sawyer, E., 1980. An alternative model for the Damara mobile belt: ocean crust subduction and continental convergence. Precambrian Res. 13, 297–336.

Basei, M.A.S., Frimmel, H.E., Nutman, A.P., Preciozzi, F., Jacob, J., 2005. A connection between the Neoproterozoic Dom Feliciano (Brazil/Uruguay) and Gariep (Namibia/South Africa) orogenic belts—evidence from a reconnaissance provenance study. Precambrian Res. 139, 195–221.

Boger, S.D., Miller, J.McL., 2004. Terminal suturing of Gondwana and the onset of the Ross-Delamerian Orogeny: the cause and effect of an Early Cambrian reconfiguration of plate motions. Earth Planet. Sci. Lett. 219, 35–48.

Briqueu, L., Lancelot, J.P., Valois, J.P., Walgenwitz, F., 1980. Géochronologie U-Pb et genèse d'un type de minéralization uranifère: les alsakites de Goanikontes (Namibie) et leur encaissant: Bull. Cent. Rech. Explor.–Prod. Elf Aquitaine 4, 759–811.

Clauer, N., Kröner, A., 1979. Strontium and argon isotopic homogenization of pelitic sediments during low-grade regional metamorphism: the Pan-African upper Damara sequence of northern Namibia (south west Africa). Earth Planetary Sci. Lett. 43, 117–131.

Clifford, T.N., 1967. The Damaran episode in the upper Proterozoic–lower Palaeozoic structural history of Southern Africa. Geol. Soc. Am. Spec. Pap., 92.

Collins, A.S., Pisarevsky, S.A., 2005. Amalgamating eastern Gondwana: the evolution of the circum-Indian Orogens. Earth Sci. Rev. 71, 229–270.

Coward, M.P., 1981. The junction between Pan African Mobile Belts in Namibia: its structural history. Tectonophysics 76, 59–73.

Coward, M.P., 1983. The tectonic history of the Damaran Belt. In: Miller, R.G. (Ed.), Evolution of the Damara Orogen of South West Africa/Namibia, 11. Geol. Soc. South Afr. Spec. Pub., pp. 409–421.

Davies, C.J., Coward, M.P., 1982. The structural evolution of the Gariep arc in southern Namibia (South-west Africa). Precambrian Res. 17, 173–198.

de Kock, G.S., Eglington, B., Armstrong, R.A., Hermer, R.E., Walraven, F., 2000. In: Miller, R.McG. (Ed.), U-Pb and Pb-Pb ages of the Naauwpoort Rhyolite, Kawakeup leptite and Okongava Diorite: implications for the onset of rifting and of orogenesis in the Damara Belt, Namibia, vol. 12. Henno Martin Commemorative Volume. Commun. Geol. Surv. Namibia, pp. 81–88.

Dürr, S.B., Dingeldey, D.P., 1996. The Kaoko belt (Namibia): part of a late Neoproterozoic continental-scale strike-slip system. Geology 24, 503–506.

Foden, J., Elburg, M.A., Dougherty-Page, J., Burtt, A., 2006. The timing and duration of the Delamerian Orogeny: correlation with the Ross orogen and implications for Gondwana assembly. J. Geol. 114, 189–210.

Foster, D.A., Gray, D.R., 2000. The structure and evolution of the Lachlan Fold Belt (Orogen) of Eastern Australia. Ann. Rev. Earth Planet. Sci. 28, 47–80.

Foster, D.A., Gray, D.R., Bucher, M., 1999. Chronology of deformation within the turbidite-dominated Lachlan orogen: implications for the tectonic evolution of eastern Australia and Gondwana. Tectonics 18, 452–485.

Foster, D.A., Gray, D.R., Kwak, T.A.P., Bucher, M., 1998. Chronology and tectonic framework of turbidite hosted gold deposits in the western Lachlan Fold Belt, Victoria: ^{40}Ar-^{39}Ar results. Ore Geol. Rev. 13, 229–250.

Foster, D.A., Gray, D.R., Spaggiari, C.V., 2005. Timing of subduction and exhumation along the Cambrian East Gondwana margin, and the formation of Paleozoic backarc basins. Bull. Geol. Soc. Am. 117, 105–116, doi:10.1130/B25481.1.

Franz, L., Romer, R.L., Dingeldey, D.P., 1999. Diachronous Pan-African granulite-facies metamorphism (650 Ma and 550 Ma) in the Kaoko belt, NW Namibia. Eur. J. Mineral. 11, 167–180.

Freyer, E.E., Hälbich, I.W., 1994. Deformation history of the lower Ugab belt. In: Niall, M., McManus, C. (Eds.), Proterozoic Crustal and Metallogenic evolution. Abstracts of the Geological Society and Geological Survey Conference of Namibia Conference, Windhoek, p. 18.

Frimmel, H.E., 1995. Metamorphic evolution of the Gariep Belt. South Afr. J. Geol. 98, 176–190.

Frimmel, H.E., 2000a. The Pan-African Gariep Belt in southwestern Namibia and western South Africa. In: Miller, R.McG. (Ed.), Henno Martin Commemorative Volume, vol. 12. Commun. Geol. Surv. Namibia, pp. 197–209.

Frimmel, H.E., 2000b. New U-Pb zircon ages for the Kuboos Pluton in the Pan-African Gariep Belt, South Africa; Cambrian mantle plume or far field collision effect? South Afr. J. Geol. 103, 207–214.

Frimmel, H.E., Frank, W., 1998. Neoproterozoic tectono-thermal evolution of the Gariep Belt and its basement, Namibia and South Africa. Precambrian Res. 90, 1–28.

Frimmel, H.E., Hartnady, C.J.H., 1992. Blue amphiboles and their significance for the metamorphic history of the Pan-African Gariep belt, Namibia. J. Met. Geol. 10, 651–669.

Frimmel, H.E., Klötzli, U., Siegfried, P., 1996. New Pb-Pb single zircon age constraints on the timing of Neoproterozoic glaciation and continental breakup in Namibia. J. Geol. 104, 459–469.

Germs, G.J.B., Gresse, P.G., 1991. The foreland basin of the Damara and Gariep orogens in Namaqualand and southern Namibia: stratigraphic correlations and basin dynamics. South Afr. J. Geol. 94, 159–169.

Goodge, J.W., Walker, N.W., Hansen, V.L., 1993. Neoproterozoic-Cambrian basement-involved orogenesis within the Antarctic margin of Gondwana. Geology 21, 37–40, doi:10.1130/0091-7613(1993)0212.3.CO;2.

Goodge, J.W., 1997. Latest Neoproterozoic basin inversion of the Beardmore Group, central Transantarctic Mountains, Antarctica. Tectonics 16, 682–701, doi:10.1029/97TC01417.

Goscombe, B., Gray, D.R., Hand, M., 2004. Variation in metamorphic style along the northern margin of the Damara Orogen, Namibia. J. Petrol. 45, 1261–1295.

Goscombe, B., Gray, D.R., Hand, M., 2005a. Extrusional tectonics in the core of a transpressional orogen: the Kaoko Belt, Namibia. J. Petrol. 46, 1203–1241.

Goscombe, B., Gray, D.R., Armstrong, R., Foster, D.A., Vogl, J., 2005b. Event geochronology of the Pan-African Kaoko Belt, Namibia. Precambrian Res. 140, 1–41.

Goscombe, B., Hand, M., Gray, D.R., 2003a. Structure of the Kaoko Belt, Namibia: progressive evolution of a classic transpressional orogen. J. Struct. Geol. 25, 1049–1081.

Goscombe, B., Hand, M., Gray, D.R., Mawby, J., 2003b. The metamorphic architecture of a transpressional orogen: the Kaoko Belt, Namibia. J. Petrol. 44, 679–711.

Gresse, P.G., 1994. Strain partitioning in the southern Gariep arc as reflected by sheath folds and stretching directions. South Afr. J. Geol. 97, 52–61.

Gresse, P.G., Germs, G.J.B., 1993. The Nama foreland basin: sedimentation, major unconformity and bounded sequences and multisided active margin advance. Precambrian Res. 63, 247–272.

Gresse, P.G., Fitch, F.J., Miller, J.A., 1988. $^{40}Ar/^{39}Ar$ dating of the Cambro-Ordovician Vanrhynsdorp tectonite in southern Namaqualand. South Afr. J. Geol. 91, 257–263.

Haack, U., 1983. Reconstruction of the cooling history of the Damara Orogen by correlation of radiometric ages with geography and altitude. In: Martin, H., Eder, F.W. (Eds.), Intracontinental Fold Belts. Springer-Verlag, Berlin, pp. 873–884.

Haack, U., Hoffer, E., 1976. K/Ar ages of biotites from the Damara orogen, South West Africa. Trans. Geol. Soc. South Afr. 79, 213–216.

Haack, U., Gohn, E., Klein, J.A., 1980. Rb/Sr ages of granitic rocks along the middle reaches of the Omaruru River and the timing of orogenic events in the Damara Belt (Namibia). Contribs. Min. Petrol. 74, 349–360.

Hälbich, I.W., Alchin, D.J., 1995. The Gariep Belt; stratigraphic-structural evidence for obliquely transformed grabens and back-folded thrust-stacks in a combined thick-skin thin-skin structural setting. J. Afr. Earth Sci. 21, 9–33.

Hanson, R.E., 2003. Proterozoic geochronology and tectonic evolution of southern Africa. In: Yoshida, M., Windley, B., Dasgupta, S. (Eds.), Proterozoic East Gondwana: Supercontinent Assembly and Breakup, vol. 206. Geol. Soc. Lond. Spec. Pub., pp. 427–463.

Hawkesworth, C.J., Gledhill, A.R., Roddick, J.C., Miller, R.McG., Kröner, A., 1983. Rb-Sr and $^{40}Ar/^{39}Ar$ studies bearing on models for the thermal evolution of the Damara Belt, Namibia. In: Miller, R.G. (Ed.), Evolution of the Damara Orogen of South West Africa/Namibia, vol. 11. Geol. Soc. South Afr. Spec. Pub., pp. 323–338.

Hoffman, P.F., Hawkins, D.P., Isachsen, C.E., Bowring, S.A., 1996. Precise U-Pb zircon ages for early Damaran magmatism in the Summas Mountains and Welwitschia Inlier, northern Damara Belt, Namibia. Commun. Geol. Surv. Namibia 11, 47–52.

Jacob, R.E., Moore, J.M., Armstrong, R.A., 2000. Zircon and titanite age determinations from igneous rocks in the Karibib District, Namibia: implications for Navachab vein-style gold mineralization. Commun. Geol. Surv. Namibia 12, 157–166.

Jung, S., Mezger, K., 2003. U-Pb garnet chronometry in high-grade rocks; case studies from the central Damara Orogen (Namibia) and implications for the interpretation of Sm-Nd garnet ages and the role of high U-Th inclusions. Contrib. Min. Pet. 146, 382–396.

Jung, S., Mezger, K., Hoernes, S., 2001. Trace element and isotopic (Sr, Nd, Pb, O) arguments for a mid-crustal origin of Pan-African garnet-bearing S-type granites from the Damara orogen (Namibia). Precambrian Res. 110, 325–355.

Jung, S., Hoernes, S., Mezger, K., 2000. Geochronology and petrogenesis of Pan-African syn-tectonic S-type and post-tectonic A-type granite (Namibia)—products of melting of crustal sources, fractional crystallization and wall rock entrainment. Lithos 50, 259–287.

Kasch, K.W., 1983a. Regional P-T variations in the Damara Orogen with particular reference to early high-pressure metamorphism along the southern margin. In: Miller, R.G. (Ed.), Evolution of the Damara Orogen of South West Africa/Namibia, vol. 11. Geol. Soc. South Afr. Spec. Pub., pp. 243–253.

Kasch, K.W., 1983b. Continental collision, suture progradation and thermal relaxation: a plate tectonic model for the Damara Orogen in central Namibia. In: Miller, R.G. (Ed.), Evolution of the Damara Orogen of South West Africa/Namibia, vol. 11. Geol. Soc. South Afr. Spec. Pub., pp. 423–429.

Konopásek, J., Kröner, S., Kitt, S.L., Passchier, C.W., Kröner, A., 2004. Oblique collision and evolution of large-scale transcurrent shear zones in the Kaoko belt, NW Namibia. Precambrian Res. 136, 139–157.

Koppers, A.A.P., 2002. Ar/Ar CALC software for 40Ar/39Ar age calculations. Comput. Geosci. 28, 605–619.

Korn, H., Martin, H., 1959. Gravity tectonics in the Naukluft Mountains of South West Africa. Bull. Geol. Soc. Am. 70, 1047–1078.

Kröner, A., 1977. Precambrian mobile belts in southern and eastern Africa—ancient sutures or sites of ensialic mobility. A case for crustal evolution towards plate tectonics. Tectonophysics 40, 101–135.

Kröner, A., 1980. Pan African crustal evolution. Episodes, 3–8.

Kröner, A., 1982. Rb-Sr geochronology and tectonic evolution of the Pan African belt of Namibia, southwestern Africa. Am. J. Sci. 282, 1471–1507.

Kröner, A., Clauer, N., 1979. Isotopic dating of low-grade metamorphic shales in northern Namibia (South West Africa) and implications for the orogenic evolution of the Pan-African Damara Belt. Precambrian Res. 10, 59–72.

Kröner, S., Konopásek, J., Kröner, A., Passchier, C.W., Poller, U., Wingate, M.T.D., Hofmann, K.-H., 2004. U-Pb and Pb-Pb zircon ages for metamorphic rocks in the Kaoko Belt of northwestern Namibia: a Paleo- to Mesoproterozoic basement reworked during the Pan-African orogeny. South Afr. J. Geol. 107, 455–467.

Kukla, C., 1993. Strontium isotope heterogeneities in amphibolite facies, banded metasediments— a case study from the Late Proterozoic Kuiseb Formation of the southern Damara Orogen. Central Namibia: Geol. Surv. Namibia Mem. 15, 139.

Kukla, C., Kramm, U., Kukla, P.A., Okrusch, M., 1991. U-Pb monazite data relating to metamorphism and granite intrusion in the northwestern Khomas Trough, Damara Orogen. Central Namibia: Commun. Geol. Surv. Namibia 7, 49–54.

McDermott, F., Harris, N.B.W., Hawkesworth, C.J., 2000. Geochemical constraints on the petrogenesis of Pan-African A-type granites in the Damara Belt, Namibia. In: Miller, R.McG. (Ed.), Henno Martin Commemorative Volume, vol. 12. Commun. Geol. Surv. Namibia, pp. 139–148.

McDougall, I., Harrison, T.M., 1999. Geochronology and Thermochronology by the $^{40}Ar/^{39}Ar$ Method, second ed. Oxford University Press, New York, 269 pp.

Maloof, A.C., 2000. Superposed folding at the junction of the inland and coastal belts, Damara Orogen, Namibia. In: Miller, R.McG. (Ed.), Henno Martin Commemorative Volume, vol. 12. Commun. Geol. Surv. Namibia, pp. 89–98.

Masberg, P., 2000. Garnet-growth in medium-pressure granulite facies metapelites from the central Damara Orogen: igneous versus metamorphic history. In: Miller, R.McG. (Ed.), Henno Martin Com-

memorative Volume, vol. 12. Commun. Geol. Surv. Namibia, pp. 115–124.

Masberg, P., Mihm, D., Jung, S., 2005. Major and trace element and isotopic (Sr, Nd, O) constraints for Pan-African crustally contaminated grey granite gneisses from the southern Kaoko belt, Namibia. Lithos 84, 25–50.

Meert, J.G., 2003. A synopsis of events related to the assembly of eastern Gondwana. Tectonophysics 362, 1–40.

Miller, R.McG., 1983. The Pan-African Damara orogen of South West Namibia/Africa. In: Miller, R.G. (Ed.), Evolution of the Damara Orogen of South West Africa/Namibia, vol. 11. Geol. Soc. South Afr. Spec. Pub., pp. 431–515.

Miller, R.McG., Grote, W., 1988. Geological Map of the Damara Orogen, Namibia (scale 1:500,000). Geological Survey of Namibia, Windhoek, 2 Sheets.

Passchier, C.W., Trouw, R.A., Ribeiro, A., Paciullo, F.V.P., 2002. Tectonic evolution of the southern Kaoko Belt, Namibia. J. African Earth Sci. 35, 61–75.

Porada, H., 1989. Pan-African rifting and orogenesis in southern to Equatorial Africa and eastern Brazil. Precambrian Res. 44, 103–136.

Porada, H., Ahrendt, H., Behr, J., Weber, K., 1983. The join of the coastal and intracontinental branches of the Damara Orogen, Namibia, South West Africa. In: Martin, H., Eder, F.W. (Eds.), Intracontinental Fold Belts. Springer-Verlag, Berlin, pp. 901–912.

Prave, A.R., 1996. Tale of three cratons: tectostratigraphic anatomy of the Damara Orogen in northwestern Namibia and the assembly of Gondwana. Geology 24, 1115–1118.

Puhan, D., 1983. Temperature and pressure of metamorphism in the Central Damara Orogen. In: Miller, R.G. (Ed.), Evolution of the Damara Orogen of South West Africa/Namibia, vol. 11. Geol. Soc. South Afr. Spec. Pub., pp. 219–223.

Seth, B., Kröner, A., Mezger, K., Nemchin, A.A., Pidgeon, R.T., Okrusch, M., 1998. Archean to Aneoproterozoic magmatic events in the Kaoko belt of NW Namibia and their geodynamic significance. Precambrian Res. 92, 341–363.

Seth, B., Okrusch, M., Wilde, M., Hoffmann, K.-H., 2000. The Voetspoor Intrusion, Southern Kaoko Zone, Namibia: mineralogical, geochemical and isotopic constraints for the origin of a syenitic magma. Commun. Geol. Surv. Namibia 12, 125–137.

Tack, L., Bowden, P., 1999. Post-collisional granite magmatism in the central Damaran (Pan-African) Orogenic Belt, western Namibia. J. Afr. Earth Sci. 28, 653–674.

Trompette, R., 1997. Neoproterozoic (∼600 Ma) aggregation of western Gondwana: a tentative scenario. Precambrian Res. 82, 101–112.

Weber, K., Ahrendt, H., Hunziker, J.C., 1983. Geodynamic aspects of structural and radiometric investigations on the northern and southern margins of the Damara Orogen, South West Africa/Namibia. In: Miller, R.G. (Ed.), Evolution of the Damara Orogen of South West Africa/Namibia, vol. 11. Geol. Soc. South Afr. Spec. Pub., pp. 307–319.